Pergamon

Geochimica et Cosmochimica Acta, Vol. 61, No. 8, pp. 1575–1594, 1997
Copyright © 1997 Elsevier Science Ltd
Printed in the USA. All rights reserved
0016-7037/97 $17.00 + .00

PII S0016-7037(97)00022-7

The albite-water system: Part III. Characterization of leached and hydrogen-enriched layers formed at 300°C using MeV ion beam techniques

ROLAND HELLMANN,[1,*] JEAN-CLAUDE DRAN,[2] and GIANANTONIO DELLA MEA[3,4]

[1]Crustal Fluids Group, L.G.I.T., C.N.R.S., Université J. Fourier, Observatoire de Grenoble I.R.I.G.M., B.P. 53X, 38041 Grenoble Cedex, France
[2]Centre de Spectrométrie Nucléaire et de Spectrométrie de Masse, Bâts. 104-108, CNRS, 91405 Campus Orsay, France
[3]Dipartimento di Ingegneria, Università di Trento, 38050 Mesiano, Italy
[4]Unità CISM-GNSM di Padova, via Marzolo 8, 35131 Padova, Italy

(*Received October* 23, 1995; *accepted in revised form January* 3, 1997)

Abstract—Samples of albite feldspar were dissolved at 300°C and 170 bars for periods up to 24 h in flow-through reactors at acid, neutral, and basic pH conditions. Three MeV ion beam techniques, Resonant Nuclear Reaction Analysis (RNRA), Rutherford Backscattering Spectrometry (RBS), and Elastic Recoil Detection Analysis (ERDA) were employed to obtain elemental depth profiles and information on the composition of the near-surface region after dissolution. Based on the anti-correlative trends of the H and Na profiles obtained by RNRA, Na loss and H permeation are coupled by an ion exchange process in acidic and neutral pH solutions. At basic pH conditions, the evidence is ambiguous as to whether there is a limited degree of ion exchange between aqueous cations and Na, as based on RBS spectra and Na RNRA profiles.

The recorded depths of H permeation and Na leaching range from a maximum at acid pH (H permeation exceeding ~10,000 Å, Na leaching ~20,000 Å) to a minimum at basic pH (no H enrichment, Na leaching depths of several hundred Å). The composition of the leached/H-enriched region is a function of pH. This is postulated to be primarily a function of two factors: the H ion concentration gradient between the solution and the solid, which directly controls the pH-dependence of the ion exchange couple H^+ (or H_3O^+) ↔ Na^+, and secondly, the speciation of ≡Al—OH and ≡Si—OH groups created by hydrolysis reactions and the subsequent preferential release of Al within the leached/H-enriched zone. Based on the ratios of H uptake to Na loss at acid and neutral pH, which range between 0.7 and 2.5, it is not possible to distinguish between H^+, H_2O, and H_3O^+ species permeating into the structure. Free water may be created within the leached/H-enriched structure via recondensation (repolymerization) reactions of adjacent ≡Si—OH groups. Excess H concentration profiles potentially provide indirect evidence for recondensation reactions at depths <700 Å during dissolution at acid pH conditions. Mass balance calculations, based on H permeation, Na loss, and Al preferential leaching, indicate that virtually no free H species (e.g., H_2O molecules) are retained in the structure after dissolution at acid pH. This result also holds true for neutral and basic pH conditions of dissolution. *Copyright © 1997 Elsevier Science Ltd*

1. INTRODUCTION

It is widely acknowledged that reactions at the fluid/solid interface play a key role in the dissolution behavior of minerals. Adsorption, ion exchange, diffusion, chelation, oxidation-reduction, bond hydrolysis, and bond repolymerization (condensation) represent some of the most important atomic-scale processes which may occur on a mineral surface during dissolution in an aqueous solution. These same processes are not necessarily restricted to the surface, however, since they also may occur within the near surface of the mineral structure, to depths ranging up to several thousands of Å. One of the direct consequences of this is the formation of an altered region between the fluid/solid interface and the unaltered bulk structure. The formation of these altered regions in many types of mineral structures and glasses is often characterized by preferential leaching and H-enrichment.

This region of near-surface alteration is of great interest to geochemists since there is increasing evidence that reactions that lead to the formation of leached and H-enriched layers are linked to the overall rate of dissolution. The H-enrichment of the near-surface region is of particular importance with respect to hydrolysis reactions since H species are considered to be the main entities involved with the breaking of framework bonds (i.e., ≡Si—O—Si≡ and ≡Al—O—Si≡ bonds in feldspars; for a theoretical treatment, see for example, Xiao and Lasaga, 1994, 1996). Thus, an understanding of the chemical and physical characteristics of the near-surface region is important for better elucidating the overall rate of dissolution, which is governed by surface detachment reactions that lead to the retreat of the fluid/solid interface.

Aside from providing important information on how fluids interact with minerals, the creation of leached/H-enriched zones during the dissolution of minerals and glasses assumes importance with respect to the geochemical mass balance of certain elements. For example, in hydrothermal submarine environments, certain heavier elements (e.g., Fe, U) and trace elements are preferentially retained within alteration layers formed on crystalline minerals and basaltic glasses

*Author to whom correspondence should be addressed (hellmann@obs.ujf-grenoble.fr).

(Petit et al., 1989b, 1990a,b; and references therein). This has importance with respect to the geochemical cycling of these elements in mid-ocean ridge environments, for example. Just as these leached and H-enriched regions are important in a natural context, they have become increasingly important with respect to environmental issues, particularly in regard to radioactive waste containment. The formation of alteration layers on rad-waste encapsulating glasses is recognized to be a potentially important means for trapping highly mobile radionuclides (e.g., actinides), thereby reducing their tendency to escape into surrounding groundwaters (Petit et al., 1990a; and references therein).

Leached layers, created by the preferential release of certain elements from the bulk mineral, have a chemical composition and structure distinct from the unaltered bulk material. The formation of leached layers is intimately associated with the pervasive influx of H species (H_2O, H^+, H_3O^+, OH^-), as well as the influx of other aqueous species from the solution into the structure. The permeation of H species into feldspars is associated with various types of reactions which consume H, such as ion exchange and framework bond hydrolysis. Since the creation of leached layers and H-enriched layers are interrelated and refer basically to the same altered mineral structure, they are referred to together in the present study.

Indirect evidence for the presence of leached and H-enriched layers in feldspars is based on the nonstoichiometric release of aqueous dissolution products (Chou and Wollast, 1984; Hellmann et al., 1990a; Stillings and Brantley, 1995; Hellmann, 1995; and references therein), as well as H charge balance calculations from dissolution and titration data (Casey et al., 1989b; Hellmann et al., 1990a). More recently, ion beam (RNRA, RBS, ERDA, SIMS) and electron spectroscopic techniques (XPS, Auger) have permitted the direct measurement of surface compositions and elemental depth profiles on glasses and minerals that have been reacted under a variety of conditions (Lee et al., 1974; Lanford et al., 1979; Berner and Holdren, 1979; Della Mea et al., 1983; Petit et al., 1987, 1989a,b,c, 1990a,b; Dran et al., 1988; Casey et al., 1988, 1989a; Hochella et al., 1988; Muir et al., 1989, 1990; Hellmann et al., 1990a,b; Shotyk and Nesbitt, 1992; Sjöberg et al., 1995, Schweda and Sjöberg, 1997). These studies show that the depletion of certain elements and the infiltration of H species can extend to depths of several thousands of Å.

The present study is the third in a series devoted to dissolution reactions in the albite-water system at elevated temperatures and pressures. The data from this study complement solution data obtained from two previous studies, the first pertaining to steady-state rates of dissolution (Hellmann, 1994; referred to as Part I), and the second pertaining to the stoichiometry of dissolution as a function of time (Hellmann, 1995; referred to as Part II). The solution data from Part II and the compositional profiles from this study provide an opportunity to directly compare fundamentally different types of measurements regarding depths of preferential leaching for samples dissolved under similar conditions. As discussed further on, the solution data are for the most part in accord with the profiles. However, there are clear quantitative differences in the two datasets.

One of the main purposes of the present study is a better understanding of the formation of leached and H-enriched layers formed during the dissolution of albite under acid, neutral, and basic pH conditions at hydrothermal temperatures. Compositional profiles and depths of these altered layers were obtained by the application of three nondestructive ion beam techniques, Resonant Nuclear Reaction Analysis (RNRA), Elastic Recoil Detection Analysis (ERDA), and Rutherford Backscattering Spectrometry (RBS). RNRA and ERDA are especially powerful tools for obtaining H profiles; in addition, RNRA is widely used for profiling Na. The RNRA and ERDA profiles yielded information on the influx and retention of H species, as well as the loss of Na (from RNRA only), to depths of analysis ranging to an approximate maximum of 10,000 Å. The RBS results served primarily to qualitatively gauge the preferential depletion of elements from the structure and the influx of aqueous species into the leached and H-enriched zone. However, precise depths of leaching and penetration could not be derived from the RBS spectra.

The direct measurement of H and Na profiles in samples reacted under various pH conditions permits a better understanding of how pH affects the loss of Na and the penetration/retention of H within the leached/H-enriched structure. The degree of H incorporation and Na loss into the structure is examined within the framework of ion exchange reactions, as well as the chemical speciation of ≡Si—OH and ≡Al—OH groups in the leached/H-enriched structure. Hydrogen and sodium measurements potentially provide the means for obtaining information on the molecular form of H species that permeate the structure. However, as will be shown further on, this approach is only valid if ion exchange is the only process occurring within the leached/H-enriched layers. Nonetheless, simple mass balance calculations to determine H consumption can be used to estimate how much H is retained as free water within the structure.

A companion article (in this issue) to the present study is based on diffusion modeling of leached/H-enriched regions (Hellmann, 1997; Part IV). The diffusion models permit a better understanding of the processes associated with leaching and H enrichment in feldspars, other similar minerals, and glasses. In addition to this, these models allow qualitative comparisons to be made with the information provided by the RNRA, RBS, and ERDA profiles and depths in Part III (this study), thereby giving a better idea of which models and which model parameters are best adapted to describing the outward diffusion of Na and the inward diffusion of H species during dissolution at steady-state conditions.

2. EXPERIMENTAL METHODS AND CALCULATIONS

2.1. Sample Preparation and Dissolution Experiments

The results presented in this study are derived from two sets of samples. A first set was prepared, reacted, and analyzed by RNRA and RBS in 1990, and a second set was prepared, reacted, and analyzed by RBS and ERDA in 1996. Both sets of samples came from the same parent sample, which is a very pure albite (chemical composition in Table 1, Part I) from Amelia Court House, VA., U.S.A. All samples were approximately 5–10 mm on a side. Samples in the first set were simply cleaved from the parent sample and extremely flat (010) surfaces were selected for the experiments. On the other hand, the second set of samples were cut from the parent sample with a diamond wire saw and natural (010) cleavage surfaces were subsequently mechanically polished with SiC paper (final pol-

ish with 800 grit). Cutting and polishing of samples was done in the presence of water. All samples were ultrasonically cleaned in either alcohol or acetone before reaction. The samples were reacted at 300°C and 170 bars for up to 24 h. The effects of shallow hydration during sample preparation could be neglected due to the rapid retreat (up to 1 Å s^{-1}) of the fluid/solid interface during dissolution at 300°C, thereby effectively removing any pre-H-enriched layer.

The first set of samples was reacted in a tubular flow-through reactor (description in Part I- Fig. 1), whereas the second set was reacted in a continuously stirred tank reactor (CSTR). The CSTR system used in this study, illustrated in Fig. 1, is composed of the following major components: a liquid reservoir, an HPLC pump, an autoclave surrounded by a furnace, a reactor control unit, and a back pressure regulator, which is used to set the pressure of the entire system. The fluid in the reservoir is pumped into the reactor, where it reacts with suspended mineral samples, and is then sampled at the outlet end of the back pressure regulator. The reactor fluid is continuously stirred with a magnetically driven impeller, thus ensuring that there are no chemical gradients within the reactor. Virtually all components in contact with fluids at elevated temperatures (autoclave, impeller, tubing, fittings) are made of high grade Ti to ensure maximum corrosion protection.

Flow systems, and CSTR systems in particular, are ideally suited for mineral dissolution studies. Their advantages over traditionally-used static autoclaves are numerous: (1) Flow systems allow for the direct measurement of the kinetics of dissolution based on the output chemistry of the solutions (see Appendix in Part I for a detailed discussion). This is perhaps their main advantage. (2) The affinity of the dissolution reaction remains constant over time during steady-state conditions of operation. (3) On the other hand, the chemical affinity can easily be increased or decreased by simply changing the residence time of the fluid in the reactor (which is dependent on the flow rate). (4) The input fluid can easily be changed (chemistry, pH, etc.) during the course of an experiment.

The measured kinetics of dissolution were the same for both types of reactors used in this study. The in-situ pH's of dissolution were 3.4, 5.7, or ~8.6–8.9 (pH values at 25°C were 3.4, 5.7, and 10.9–11.3, respectively). The pH's of fluids at the inlet and outlet of the reactor were constant, to within ±0.2 pH units. The acidic and basic solutions were pH-adjusted with HCl and KOH or $Ba(OH)_2$, respectively. In addition, no background electrolytes were used, except in one case (sample E17).

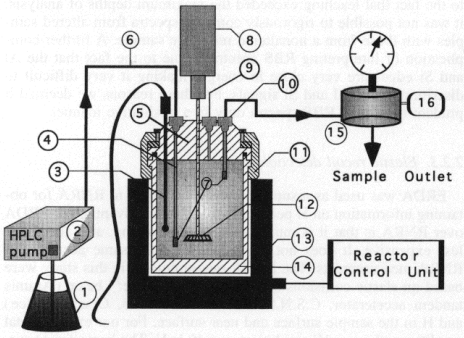

Fig. 1. Hydrothermal flow system incorporating a *c*ontinuously *s*tirred *t*ank *r*eactor (CSTR). The individual components are as follows: (1) fluid reservoir, (2) high precision HPLC pump (Knauer® series 64), (3) well for J-type thermocouple, (4) inlet tubing (Ti), (5) reactor head, (6) 1/8'' Ti tubing, (7) 5 μm Ti filters, (8) magnetic stirrer housing, (9) burst disk assembly, (10) Ti Swagelok® fittings, (11) split ring, (12) impeller, (13) furnace, (14) Ti autoclave, 300 mL volume (Parr® 4560 series), (15) back pressure regulator (Grove Mity Mite® S91XW), and (16) high pressure gas source.

The attainment of 300°C without any temperature overshoot generally took 1.7–2 h. At the end of a given experiment, samples were recovered relatively rapidly. This was possible by gradually opening the back pressure regulator to atmospheric pressure and letting some of the solution escape as steam. On average, ten minutes passed between experimental conditions at P and T and the attainment of ~90°C conditions, which permitted the recovery of the samples. After removal from the reactor, the samples were rinsed in water and then stored in air for several weeks before the various ion beam analyses were done.

The 24 h reaction time of the samples is representative of steady-state dissolution conditions. This is based on the attainment of steady-state concentrations and the stoichiometry of Na, Al, and Si in the outlet solutions (see extensive dataset in Part II, which shows that steady-state conditions were generally achieved in less than 5 h at 300°C). The dissolution reactions were run at conditions far from equilibrium. The chemical affinities were calculated using the geochemical code EQ3 (Wolery, 1992), based on the solution chemistry at the end of the experiments. The first set of samples had chemical affinities ranging from 69 to 123 kJ mol^{-1}; for the second set of samples, the affinities ranged from 98 to 140 kJ mol^{-1}. The chemical affinities, as well as rates, concentrations, etc. for the samples from the first set (RD, RC, and RE) can be found in Table 3, Part I. The interested reader desiring more information with respect to these samples, experimental conditions, methods, and calculated rates, affinities, etc. used in this study should refer to Parts I and II.

2.2. Ion Beam Techniques

Three MeV ion beam techniques were utilized, Resonant Nuclear Reaction Analysis (RNRA), Rutherford Backscattering Spectrometry (RBS), and Elastic Recoil Detection Analysis (ERDA). Only a brief description of these techniques will be given here.

2.2.1. Resonant nuclear reaction analysis

The RNRA analyses were performed with the Legnaro accelerators (INFN, Padova, Italy). For all samples, only (010) surfaces were analyzed (note: (010) and (001) are the dominant cleavage planes in albite; Deer et al., 1978). The RNRA technique is based on a nuclear reaction between a monoenergetic ion beam and an isotope of a given element. As the ion beam penetrates the solid, its energy is attenuated as a function of depth, due mainly to electronic collisions. The rate of energy loss, dE/dx, is a function of the stopping power of the material. Eventually, a depth is reached corresponding to the resonance energy, where an element-specific nuclear reaction takes place at a certain narrow energy band. The alpha particles and gamma rays produced by the nuclear reaction are directly proportional to the concentration of a specific isotope at that given depth. Stepwise increases in the energy of the incident beam increase the depth at which this nuclear reaction takes place, thereby providing a depth profile for the isotope of interest. The RNRA technique is especially well-suited for profiling light elements (atomic numbers 1–~20), such as H and Na. Maximum depths of analysis of approximately 10,000 Å can be attained with this technique. More details on RNRA, as applied to similar geochemical problems, can be found in Petit et al. (1990a,b), and references therein; more specific details with respect to RNRA can be found in Amsel and Lanford (1984) and Cherniak and Lanford (1992).

The concentration of H was measured as a function of the emission of γ rays according to the following resonant nuclear reaction: $^{1}H + {}^{15}N \rightarrow {}^{12}C + {}^{4}He + \gamma$. This reaction has a 6.385 MeV resonance energy and a width of 1.8 keV (Petit et al., 1990b). In silicates, the depth resolution is approximately 30 Å at the surface and 100 Å at 1000 Å depth (Della Mea et al., 1983). The experimental beam conditions for H profiling were as follows: energy resolution of $^{15}N^{2+}$ beam ~ 4 keV, 3 mm^2 beam size and 1.5 $\mu A\ cm^{-2}$ intensity, energy step size ~ 15 keV corresponding to ~ 80 Å depth. Calibration was effected by analyzing H-implanted Si samples as well as natural hornblende samples.

Depth profiles of Na were obtained by measuring emitted α particles, based on the following nuclear reaction: $^{23}Na + {}^{1}H^{+} \rightarrow {}^{20}Ne + {}^{4}He$. This reaction has a 592 keV resonance, a width of 0.6 keV (Petit et al., 1990b), and a resolution of 100 Å at the surface for

common silicates (Della Mea et al., 1983). The experimental beam conditions for Na profiling were as follows: ~1 mm^2 beam size and 1 $\mu A\ cm^{-2}$ intensity, energy step size ~ 1 keV corresponding to ~150 Å depth. Calibration consisted of analyzing a NaCl crystal. For both types of analyses, samples were carbon coated to avoid charging effects.

Due to the time consuming and costly nature of the RNRA technique, replicate samples were not analyzed for each pH condition. However, we were able to directly compare these RNRA results with those obtained for albite glass samples (prepared from the same parent samples) that were reacted under the same experimental conditions (R. Hellmann, unpubl. results). The H concentration profiles at acid and basic pH are similar (within 10–15%) to the results for crystalline albite. The amorphous albite reacted at neutral pH shows a significantly higher degree of H enrichment, however. The Na concentration profiles for amorphous and crystalline albite are similar for all pH conditions of dissolution. This comparison serves to show that the RNRA results presented in this study are in fact representative. In addition, sample heterogeneity is not expected to have a major influence on the results since each analysis (beam spot sizes are on the order of several mm^2) represents a significant fraction of the total surface area of the sample.

Overall, the accuracy of elemental analyses by RNRA is on the order of 10–20%, depending on the concentration of the element analyzed, sample preparation techniques, etc. (for more details, see Petit et al., 1990a). In the present study, propagation of error calculations applied to the RNRA data are based on an estimated error of ±10% for concentrations at depths < 1000 Å, ±20% at depths > 5000 Å, and ±15% at intermediate depths. This variation in uncertainties reflects a decrease in the accuracy of measurements with depth (see Dran et al., 1988 for details). In addition, it should also be noted that shallow near-surface RNRA analyses should be interpreted with caution since the stopping power is dependent on elemental concentrations that are often poorly constrained at the surface (Petit et al., 1990a).

Even though there was no direct evidence that the measured H and Na RNRA profiles were indeed invariant with time, the results at 300°C from Part II show that the release rates for Na, Al, and Si reach steady-state over periods of time on the order of 5 h or less. In addition, the analysis of the output pH in another similar dissolution study (Fig. 10 of Hellmann et al., 1990a) shows that steady-state H consumption also was achieved over similar timescales. Based on this evidence, the H and Na profiles presented in this study are considered to represent the steady state.

2.2.2. *Rutherford backscattering spectrometry*

RBS and ERDA are both techniques that are based on the interaction of a beam of light ions with a sample surface. In the case of ERDA, the energy spectrum of forward recoiled $^1H^+$ ions is measured, whereas RBS is based on the measurement of the energy spectrum of backscattered ^4He ions. A schematic view showing the geometry of the incident beam, the sample surface, and the resulting forward recoiled and backscattered ions used in this study is illustrated in Fig. 2.

Considering RBS first, this technique is specifically based on Coulombic interactions between He^+ ions of the beam and the nuclei of atoms at the surface and near surface. These collisions result in elastic backscattering of a small proportion of the incident He ions. Since the number of backscattered He ions is proportional to the square of the atomic number of the target material, RBS is especially suited for heavier elements. The backscattered He ions are analyzed in energy, which is in effect a mass discrimination of the target nuclei. This is due to the fact that collisions with a heavy element impart a greater energy to backscattered He ions than similar collisions with a lighter element. The RBS energy spectrum consists of specific energy edges and steps, with each edge occurring at a defined energy and corresponding to a specific element. The height of a specific step is a function of the surface concentration of a given element (and other instrumental factors), whereas the energy distribution around each edge provides information on the concentration with depth. For a review of this technique as applied to similar geochemical studies, see Casey et al. (1988, 1989a) and Petit et al. (1990a,b); for more detailed general information on RBS, see Chu et al. (1978).

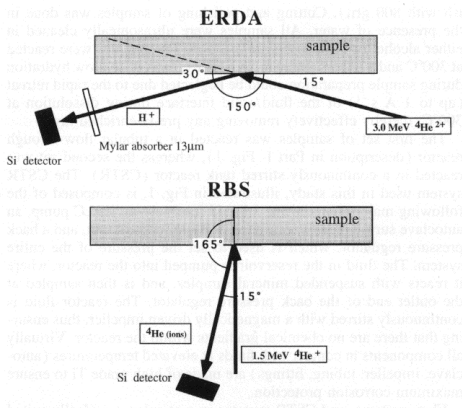

Fig. 2. Geometrical configurations of the ion beam, sample, and detector used to measure forward recoiled H^+ ions (ERDA) and backscattered ^4He ions (RBS).

The samples from this study were analyzed at the Aramis tandem accelerator (C.S.N.S.M., C.N.R.S.-IN2P3, Orsay, France) with a 1.5 MeV $^4He^+$ beam and a spot diameter of ≈1 mm. The geometry of the incident beam, the target, and the backscattered ions is given in Fig. 2. The Si detector has a resolution of 15 keV. The depth resolution is ~100 Å, which is in general inferior to the resolution for the same element analyzed by RNRA. The maximum depth of analysis is on the order of 2 μm (20,000 Å).

The quantitative determination of elemental concentrations as a function of depth is normally done by comparison between experimental and synthetic RBS spectra, which are based on first principles and assumed target composition (e.g., using the code RUMP). However, in the present study, a quantification of depths by comparison with synthetic spectra was not defensible without more detailed a priori information on the composition of the leached/H-enriched layers over the probed depth of analysis (~2 μm). In addition, due to the fact that leaching exceeded the maximum depths of analysis, it was not possible to rigorously compare spectra from altered samples with those from a nonaltered reference sample. A further complication of interpreting RBS spectra is due to the fact that the Al and Si edges are very close in energy, making it very difficult to discriminate the Al and Si signals. For these reasons we deemed it prudent to use the RBS spectra only in a qualitative manner.

2.2.3. *Elastic recoil detection analysis*

ERDA was used as a supplementary technique to RNRA for obtaining information on H penetration. The main advantage of ERDA over RNRA is that it is much less time consuming, and, therefore, less expensive. It does not, however, offer the same accuracy as RNRA measurements. The ERDA measurements in this study were based on elastic collisions between a 3.0 MeV He^{2+} beam (Aramis tandem accelerator, C.S.N.S.M., C.N.R.S.-IN2P3, Orsay, France) and H in the sample surface and near surface. For our experimental conditions, the overall resolution was 40 keV. The beam-target surface and the target surface-detector angles are illustrated in Fig. 2. The area of analysis is approximately 4 × 5 mm. Hydrogen concentrations as a function of depth are determined by the stopping power of albite for He and H ions, and the energy spectrum of recoiled $^1H^+$. The calibration of measured H concentrations is routinely done by analysis of two reference standards, Si containing a precise concentration of implanted H (10^{17} atoms cm^{-2}) and a $SiGe_2$/SiO_2 compound, where the 4,000 Å thick $SiGe_2$ layer contains 14% H (calibrated by RNRA). Both ERDA and RBS measurements were made in a vacuum of 10^{-7} torr. For more detailed information on

ERDA, see Tirira et al. (1990) and Barbour and Doyle (1995); for various applications in geochemistry, see for example Bunker et al. (1983), Casey et al. (1988, 1989a), Sweeney et al. (1997); and references therein.

Due to the fact that ERDA is based on a shallow angle of ion beam incidence with the sample surface (15°), the quality of the results is very sensitive to surface rugosity. Even though the initial sample surfaces were extensively polished, the surfaces after the dissolution runs could not be repolished, since this would have destroyed the acquired H depths profiles. It appears that surface rugosity, due to etch pits and other corrosion features, had a deleterious effect on the energy spectra collected for all of our samples. In addition, as is the case for RBS, the rigorous interpretation of ERDA spectra depends on a relatively accurate a priori knowledge of the stoichiometry of the target material (i.e., the leached/H-enriched zone). Because of these two reasons, we have used the ERDA results in a qualitative manner that simply permits us to estimate depths and to compare relative degrees of H-enrichment for various pH conditions of dissolution.

3. RESULTS AND COMPARISONS WITH OTHER STUDIES

3.1. RNRA

3.1.1. Hydrogen profiles

Hydrogen profiles for an unaltered sample and samples subjected to dissolution at acid, neutral, and basic pH are shown in Fig. 3. The unreacted sample shows a monotonic decrease in [H] from $\sim 2 \times 10^{21}$ atoms cm^{-3} at the surface to ~0 at a depth of ~600–1000 Å. Similar depths of penetration have been reported for unreacted albite by Petit et al. (1989b) and labradorite by Casey et al. (1988, 1989a). These results show that moderately shallow H penetration in the near-surface structure of feldspars occurs as a natural consequence of exposure to air.

At acid pH (3.4), the H profile shows a relatively constant concentration plateau of $\sim 8-9 \times 10^{21}$ atoms cm^{-3} over a depth range of 6000 Å. The entire depth of H penetration is beyond the analytical limits of these particular RNRA analyses; we can only assume a sharp decrease in H at some depth > 6000 Å. It is noteworthy that the H concentrations remain almost an order of magnitude greater than those recorded for an unaltered sample over a depth of more than 6000 Å. These elevated, plateau-like H concentrations are indicative of the pervasive penetration of H species of the near-surface structure during dissolution at acid pH. A SIMS study of labradorite dissolved at 25°C and acid pH produced very similar H plateau values, in the range of $1.0-2.3 \times 10^{22}$ atoms/cm^3, and depths of H penetration on the order of 2000 Å at pH 3–6000 Å at pH 1 (Schweda and Sjöberg, 1997). Results from Casey et al. (1988, 1989a), based on the dissolution of labradorite at pH 3.0 and 25° or 45°C, are similar to those of Schweda and Sjöberg (1997), except that the concentrations of H close to the surface are ~65% less. In both cases, the total amount of H incorporated was significantly less than was found in albite in the present study. This is due to a convolution of several factors: temperature, mineral composition, and structure.

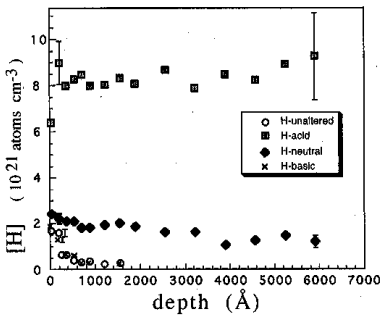

Fig. 3. Hydrogen concentrations measured by RNRA as a function of depth. The H plateaus at acid and neutral pH denote the pervasive infiltration and retention of H species deep within the leached/H-enriched structure, beyond the depth limit of the RNRA measurements. Note the strong pH-dependence of H incorporation: $[H]_{acid\ pH} > [H]_{neutral\ pH} > [H]_{basic\ pH} \approx [H]_{non\text{-}altered}$.

The H profile for a sample dissolved at neutral pH (pH 5.7) shows a decreasing, approximately linear trend extending from the surface to a depth of 6000 Å. At this depth there is still a significant amount of H ($\sim 1.5 \times 10^{21}$ atoms cm^{-3}) present within the structure. The overall H concentrations as a function of depth are almost an order of magnitude less than those obtained at acid pH. The results of Casey et al. (1989a) for labradorite dissolution at near neutral conditions (pH 5.0 and 7.0) at 45°C also show that the depth of H penetration into the structure is much less than what they recorded at acid pH (pH 1–3). Results obtained by Petit et al. (1989a,b) for the dissolution of albite at neutral pH show the important effect of temperature; the penetration depths and the total amount of H incorporated into the structure at 100° were far less than at 200°C, and in turn, these values were significantly less than those measured at 300°C in the present study.

It is interesting to note that Petit et al. (1989c) found that levels of H in the shallow near surface (to depths of ~500 Å) decreased by a factor of 2 with respect to the original concentrations as a function of time during dissolution at 100°C and neutral pH conditions. They suggested that this effect was probably due to the dissolution of an initial surface structure which may have been damaged during sample preparation. On the other hand, a study by Casey et al. (1988) showed that H levels increased in the near-surface structure of labradorite as a function of time during dissolution at acid pH. These results point out that the initial structural state of the surface region plays a potentially important role in determining the initial influx of H species into the leached/H-enriched zone. This problem also points out an inherent advantage to dissolution carried out at elevated temperatures (e.g., 300°C in the present study). Since dissolution rates at elevated temperatures are high, any surface artifacts or abnormally high levels of hydration created during sample preparation are removed by the rapid retreat of the fluid/solid interface (at pH 3.4 and 300°C, the rate of retreat is ~1 Å s^{-1}).

The sample dissolved at basic pH (8.6) has a H profile indistinguishable from that of the unreacted sample. This result was also shown by Casey et al. (1988, 1989a). The fact that H concentrations in samples reacted at basic pH are not greater than those in a nonaltered sample suggests (at least) one of two possibilities: either H species do not participate in dissolution reactions within the near surface or, alter-

natively, H species are present during dissolution but are not retained within the structure. These ideas are developed later on.

The most significant finding from the results in the present study, as well as from the previously published results discussed above, is that the temperature and the pH of dissolution control to a large degree the total amount of H incorporated in the leached/H-enriched zone. In general, the total amount of H in the structure increases by orders of magnitude as the temperature is increased from 25 to 300°C. It is, however, important to note that the total incorporation of H at any temperature is a function of pH, since the amount of H incorporation decreases with increasing pH. Under moderate to very basic pH conditions, there is no apparent temperature dependence, since reacted samples do not contain more H than is present in unreacted samples. Possible reasons for this pH dependence are discussed later on.

3.1.2. *Sodium profiles*

Using the same samples analyzed for H, Na concentrations were measured by RNRA; these data are shown in Fig. 4a. The unaltered reference sample yielded a nearly constant Na concentration of $\sim 6 \times 10^{21}$ atoms cm^{-3}. This is the amount theoretically present in the bulk material, based on published crystallographic data (4 Na atoms per unit cell volume of 664.5 $Å^3$; Harlow and Brown, 1980). The sample dissolved at acid pH shows almost complete Na depletion up to a depth of ~500 Å, beyond which the Na data show a sigmoidal increase, marked by an increase in concentration by approximately a factor of 3. This is followed by the attainment of a relatively constant plateau of $\sim 2 \times 10^{21}$ atoms cm^{-3}. This concentration plateau represents only one third of the amount of Na found in unaltered albite, thereby suggesting that Na depletion extends to significant depths, potentially much further than the analytical limits of the RNRA technique (~10,000 Å). It is interesting to note that similar behavior was noted with XPS profiles of albite samples altered at 225°C (Hellmann et al., 1990a). Even though it cannot be proven, it is quite likely that the Na concentrations increase in a sigmoidal manner before the attainment of Na levels commensurate with the unaltered material (examples of sigmoidal behavior can be noted in several studies: Casey et al., 1988, 1989a; Petit et al., 1989b, 1990b; Schweda and Sjöberg, 1997).

Dissolution at neutral pH resulted in Na concentrations slightly more than half of that measured in the unaltered sample. A slight sigmoidal increase in Na concentrations, from ~3 to 4×10^{21} atoms cm^{-3}, also occurs over approximately the same depth range as the more pronounced sigmoidal increase measured at acid pH. As was the case at acid pH, the overall degree of Na loss appears to be very significant and probably extends many thousands of Å into the structure. Judging from the Na profile in albite presented in Petit et al. (1989b), the degree of Na loss can be quite variable from sample to sample. Their results for dissolution at 200°C and neutral pH show almost complete removal of Na to a depth of approximately 1000 Å. This degree of extensive Na removal was only observed for dissolution under acid pH conditions in the present study.

The sample reacted at basic pH has a profile indicating a

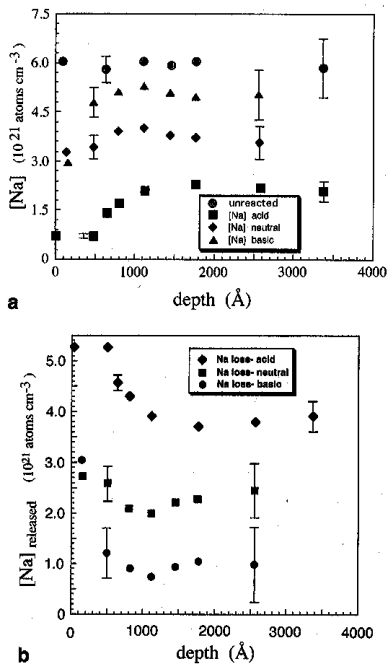

Fig. 4. (a) Sodium concentrations measured by RNRA as a function of depth. As with H incorporation, [Na] present in the leached/H-enriched structure displays a strong pH-dependence. The anticorrelative trend between H infiltration and Na retention implies ion exchange between H^+ (or H_3O^+) and Na^+. As was also the case with H, the Na measurements indicate that the depths of depletion at acid and neutral pH exceed the probed thickness. (b) Na release (i.e., loss) as a function of depth, which is defined as: $\Delta Na_{released} = [Na]_{bulk} - [Na]_{measured}$. Note the strong degree of Na loss at the very near surface, especially at acid pH.

significant amount of Na loss up to a depth of ~500 Å, with a Na concentration at the surface approximately equal to that measured at neutral pH. At greater depths the Na profile is relatively constant, on the order of $\sim 0.6 \times 10^{21}$ atoms cm^{-3} less than that of the unaltered sample. This difference may not be significant since it falls within the range of analytical uncertainty of the measurements.

The overall pH-dependence of Na depletion is represented in a slightly different manner in Fig. 4b. This figure shows Na depletion ($\Delta Na_{released}$) as a function of depth, where depletion for a given pH and depth is defined as: $\Delta Na_{released} = [Na]_{bulk} - [Na]_{measured}$. The Na depletion curves at acid and neutral pH clearly show an abrupt change in behavior in the region ranging from the surface to depths of ~1000–1500 Å. This may be indicative of a much greater degree of Na loss close to the surface as compared to regions beyond 1500 Å in depth. It is interesting to note that the Na loss at shallow depths within the near-surface structure at basic pH is roughly equal to that recorded at neutral pH. At greater depths, however, the Na depletion profile at basic pH de-

creases more rapidly. The degree of Na loss at depths greater than 1000 Å is on the order of 1.0×10^{21} atoms cm^{-3}. However, additional analyses would be needed to ascertain whether Na loss at depths beyond 1000 Å is a real phenomenon.

One of the most important results shown by the Na trends in Fig. 4a,b is that the degree of Na depletion within the leached/H-enriched region decreases as a function of increasing pH. The anti-correlative trends between Na and H are strong evidence for ion exchange between Na^+ and H^+ or H_3O^+. In addition, the nature of the H and Na profiles suggests the interdiffusion of Na and H species (Petit et al., 1989b). The results of Petit et al. (1989b) also show that the release of Na is effectively suppressed when albite is dissolved in a Na-spiked solution. These results point out the overall importance of the rate of diffusion in determining the degree of Na loss. The interrelated nature of H and Na diffusion and ion exchange is discussed in detail in Part IV.

3.2. RBS

In the following section several RBS spectra are shown for samples altered at acid, neutral, and basic pH conditions. As was the case for the RNRA analyses, only (010) surfaces were analyzed. Figure 5a shows a comparison of the spectra for a natural cleavage surface and that of a polished surface. Note that the spectra overlap within the energy ranges corresponding to the Na, Al, and Si edges. This result indicates that the polishing procedure detailed earlier does not lead to a detectable depletion of these elements. Figure 5b shows a close-up of a spectrum for the same natural cleavage surface compared to a fitted theoretical RBS spectrum (the stoichiometries that were used for the synthetic spectrum are given in the figure caption). It is interesting to note that the RBS spectrum reveals the presence of either Ca or K. Based on the fitted theoretical spectrum, the molar concentration of K or Ca with respect to Na is ~0.015:1.0 (note that the K and Ca edges are very close in energy, and, therefore, these elements cannot be easily discriminated; henceforth they are referred to together as K (Ca)). These results may indicate the presence of plagioclase or K-feldspar micro-domains, respectively. The spectrum also reveals the presence of trace amounts of Fe (either an in situ impurity or from Ti reactor) and Au (contamination from metal coating evaporator). The sharp drop in the Au spectrum with decreasing energy indicates only a surficial enrichment in Au.

Figure 6a shows the RBS spectra for two samples that were reacted at pH 3.3 and 300°C for periods of 3 and 24 h (samples E11 and E5, respectively). These spectra are compared with a reference spectrum for a nonaltered, polished sample (sample NP). Based on the reasons given previously, exact elemental depths of leaching based solely on the RBS spectra cannot be determined. Nonetheless, examination of the spectral step heights and yields associated with the Si, Al (not shown for clarity), Na, and O edges reveals that the altered samples can be characterized by zones of leaching that do not have the same stoichiometry as the nonaltered reference. The depths associated with this alteration extend beyond the limits of analysis (≈ 2 μm).

Figure 6b represents two close-ups of the same spectra, showing replicate analyses of E11 (left side of figure) and E5

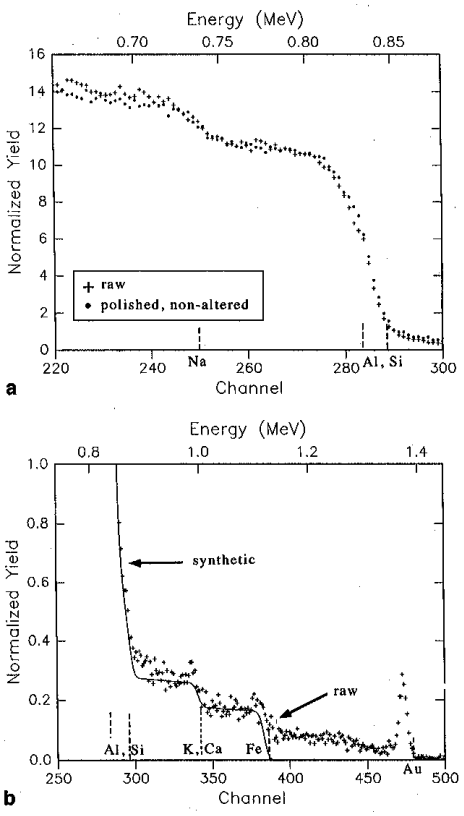

Fig. 5. (a) RBS spectra for two nonreacted surfaces, a natural cleavage surface and a polished surface. The RBS spectra show the normalized yield of backscattered ^4He ions as a function of their kinetic energy. The spectra consist of steps associated with characteristic edges for Si, Al, and Na that are located at specific energies. The overlap in the spectra indicate no significant differences in Si, Al, and Na concentrations between the samples. (b) RBS spectrum of the same natural cleavage surface in (a) and a fitted synthetic spectrum, based on the following stoichiometry for pure albite that contains minor impurities and a surficial layer of C: Fe 0.018, K (Ca) 0.015, Si 3.00, Al 1.00, Na 1.00, O 8.00, C 1.00. The constant vertical offset (i.e., step height) associated with the K or Ca edge suggests the presence of K-feldspar or plagioclase micro-domains to significant depths. Note that the proximity of the K and Ca edges does not allow for the discrimination of these elements.

(right side of figure), and two reference spectra, nonaltered sample NP and a synthetic spectrum based on the stoichiometry of albite. The spectra of the altered samples clearly show the lack of discernible Na edges as compared to the Na edges present for the references. Note also that the spectra show smooth increases in the normalized yield at energies below the respective Na edges; these spectra also remain roughly equidistant from those of the reference spectra (Fig. 6a). This indicates that the alteration zones associated with

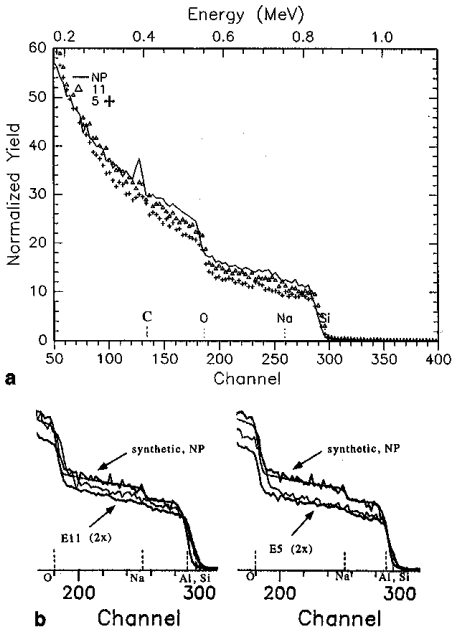

Fig. 6. RBS spectra for two altered samples at acid pH (E11 reacted for 3 h; E5 reacted for 24 h), compared to a nonaltered sample (NP). (a) The full RBS spectra show that the Si, Al, Na, and O stoichiometries of the altered samples are different from that of the reference sample over the entire probed thickness (~2 μm). (b) Close-ups of two replicate spectra (E11 on the left and E5 on the right), compared to NP and an additional synthetic spectrum representing pure albite (smooth line). The lack of Na edges and the continuous nature of the E11 and E5 spectra suggest depletion of Na over the entire probed thicknesses (~2 μm). In addition, the lower yield associated with the Al and Si edges in E5 vs. E11 (as compared to the two reference spectra) is interpreted to indicate a greater degree of Al leaching in E5 (see text for details).

E11 and E5 have a relatively constant composition and that Na depletion occurs to depths exceeding the probed thickness (~2 μm). In addition, it is interesting to note that the relative difference (with respect to the reference spectra) in the step height of the E5 spectrum at the Al and Si edges is noticeably less than that of E11, which was reacted for a much shorter period of time. The RBS spectra themselves do not allow for a quantification of this behavior, since step heights are can vary from one sample spectrum to another. However, evidence from solution analyses (see discussion further on, see also Part II), as well as data in the literature concerning near-surface depth profiles measured on altered albites, as well as other feldspars (e.g., Casey et al., 1989a; Hellmann et al., 1990a), suggest that the decreased step heights and yields at energies below the Al, Si edges of sample E5 vs. E11 can be attributed to a greater degree of preferential Al loss having occurred in E5, which was reacted for a significantly longer period of time.

Figure 7 shows the spectra for two samples that were reacted at neutral pH and 300°C (E8 for 1 h and RC for 24 h), and the spectrum for the nonaltered sample NP. The step heights corresponding to the Si (and Al), Na, and O edges are very similar. The cause for the shift in the RC spectrum towards higher energies near the Si edge is not known. The close similarity of the spectra corresponding to the altered and reference samples indicates similar stoichiometries, within the accuracy and sensitivity of the analyses. In comparison with the results deduced from Fig. 6a,b, the degree of alteration (i.e., preferential leaching) at neutral pH conditions is significantly less than that at acid pH.

Despite the lack of evidence for significant Na leaching and H enrichment at basic pH conditions (see RNRA results, Figs. 3, 4a,b), several experiments were run to examine whether altered zones, characterized by the exchange of leached constituents with aqueous cations, also occur at basic pH conditions. Results for two samples altered at basic pH conditions are shown in Fig. 8. The first sample, E16, was dissolved in a degassed, 1.3×10^{-3} M $Ba(OH)_2$ solution (pH 8.6 at 300°C; pH = 11.3 at 25°C). The RBS spectrum at the Ba edge illustrates the effect of a significant Ba surface precipitate (the presence of which was verified by SEM). Based on the chemistry of the aqueous solution and saturation indices calculated with the code EQ3, the precipitate may be a Ba silicate (i.e., $Ba_2Si_3O_8$ or Ba_2SiO_4). However, there may well be a possible incorporation of Ba into the structure as well. If Ba were only present as a thick surface precipitate, the Si and Al edges would have been shifted to lower energies; this however, is not observed (see Fig. 8). We interpret this complex spectrum as representing a probed surface that was partially coated with a Ba precipitate, but that some of the surface was also free of precipitate. Even though the general shape of the spectrum roughly parallels that of the nonaltered reference sample, the Ba signal renders the accurate measurement of step heights associated with the Al, Si, and Na edges very difficult.

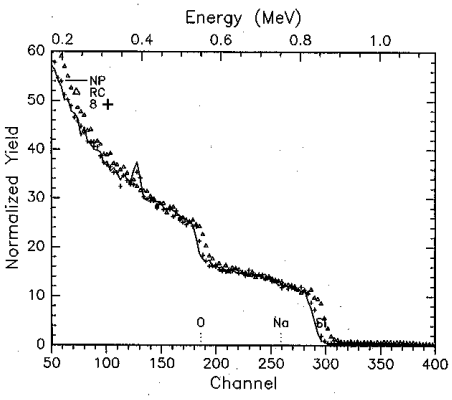

Fig. 7. RBS spectra for two altered samples at neutral pH (E8 reacted for 1 h, RC reacted for 24 h), compared to a nonaltered sample (NP). The close similarity in the spectra suggest negligible differences in the Si, Al, Na, and O stoichiometries. Comparing these RBS results to those in Fig. 6a suggests significantly less alteration occurs at neutral vs. acid pH.

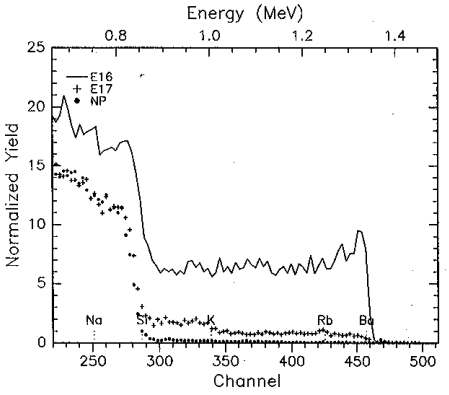

Fig. 8. RBS spectra for two samples altered at basic pH conditions, compared to a nonaltered sample (NP). E16 was altered in a 1.3 $\times 10^{-3}$ M $Ba(OH)_2$ solution. Its spectrum reveals a large vertical offset, starting at the Ba edge. We interpret this complex spectrum as representing a probed surface that was partially coated with a Ba precipitate, but that some of the surface was also free of precipitate (see text for details). Sample E17 was altered in a 10^{-3} M KOH, $\sim 4 \times 10^{-3}$ M RbCl solution; after alteration there was no evidence for the same degree of precipitation encountered with E16. The vertical offset associated with the K edge (or Ca edge, which is not shown for clarity) is interpreted to be due to the near-surface enrichment of K (compare this normalized yield with that in Fig. 5b).

A second sample (E17) was altered in a degassed, 10^{-3} M KOH, $\sim 4 \times 10^{-3}$ M RbCl solution (pH 8.3 at 300°C, pH 11.0 at 25°C). The composition of this solution avoided the significant precipitation of a secondary phase during dissolution. The broad and flat extent of the yield at energies below the K (Ca) edge is indicative of the presence of K (Ca) to significant depths, but that cannot be quantified, however. Note that the yield of K (Ca) is significantly greater than that measured for the nonaltered reference sample (see Fig. 5b). The step height associated with Rb is too small to verify its presence and depth extent within the near surface. Due to presence of K (Ca), the spectrum of E17 has been shifted upwards, starting from the K (Ca) edge (see Fig. 8). This upward shift influences the interpretation of the Si, Al, Na, and O step heights. Subtraction of the K (Ca) step height, for example, decreases the Al and Si step heights with respect to the nonaltered reference, thereby suggesting a depletion of Al and/or Si. However, the qualitative nature of the RBS spectra do not allow us to quantify this.

The question arises as to what the K (Ca) spectra represent. The presence of K or Ca within the near surface may be due to microdomains of K-feldspar or plagioclase, respectively, as was shown in Fig. 5b, which shows that K (Ca) is present in minor quantities in samples that are nonpolished and nonaltered. Upon alteration, significant enrichment of K (Ca) occurred in all samples that were reacted at basic pH in KOH/H_2O solutions, while no enrichment was noted in samples altered at acidic or neutral pH (with one notable exception at neutral pH– possibly due to contamination?). The omnipresence of a K (Ca) signal in samples altered at basic pH conditions suggests that K from the aqueous solution may have penetrated the structure. The presence of a K-bearing precipitate is unlikely, based on saturation index calculations. Supporting evidence for this is based on the observation that the Si and Al edges did not shift to lower energies (see Fig. 8).

One possible mechanism for the incorporation of K into the structure is via the ion exchange couple: $K^+ \leftrightarrow Na^+$. Clear evidence for measurable Na depletion in the RBS spectra of samples E16 and E17 is lacking, however. Close-up examination of spectrum E17 reveals the presence of a Na edge. Nonetheless, the RNRA results presented in Fig. 4a show that there is some shallow loss of Na from the albite structure upon alteration at basic pH conditions, to depths of ~500–1000 Å (see also XPS results in Hellmann et al., 1990a). This result shows that a minor amount of $K^+ \leftrightarrow Na^+$ exchange may be possible. Another possibility that can be considered is that K^+ serves to charge balance $\equiv Si—O^-$ and $\equiv Al—O^-$ groups created by the hydrolysis and preferential loss of Al from the altered zone (see Eqn. 5 and discussions further on). Direct evidence for the preferential loss of Al in this study is missing, though we can speculate that this is possible, based on the discussion above pertaining to the RBS results in Fig. 8. In addition, the solution results in Part II do show that Al loss occurs at elevated basic pH conditions and 300°C.

3.3. ERDA

The results that were obtained by ERDA are based on the second set of albite samples, as was the case for the RBS spectra presented in Figs. 5–8. Sample RC is the one exception since it belonged to the first set of samples, but it was also analyzed by ERDA and RBS along with samples of the second set. Figure 9 shows the ERDA spectra of four samples (010 surfaces): NP, nonaltered; RC, altered at neutral pH for 24 h; E8, altered at neutral pH for 1 h; E5, altered at pH 3.3 for 24 h. The spectra shown were not quantitatively treated further for two reasons: First, the spectra are of poor quality, most probably due to the deleterious effects of post-reaction surface rugosity. Secondly, as was the case for RBS, a quantification of depths by comparison with synthetic spectra was not defensible without more detailed a priori information on the composition of the leached/H enriched layers. Nevertheless, some important qualitative information was extracted from the spectra shown in Fig. 9.

The nonaltered sample NP (surprisingly) presented by far the greatest normalized yield of H, but the depth of penetration is below the resolution of the technique, and is, therefore, restricted to depths less than 1000 Å. It is not certain why this nonaltered sample had such an elevated concentration of surficial H (compare to nonaltered sample in Fig. 3). The relative differences in H between this sample and the reacted samples may be due in part to the extreme flatness of the unreacted surface, this leading to a higher signal/noise ratio (in particular at the surface). Another reason is based on enhanced H incorporation into a damaged surface structure created during the polishing process. However, as mentioned earlier, the rapid retreat of the surface during dissolution (1 Å s^{-1} at pH 3 and 300°C) ensures that any surficial hydration present at the start of an experiment has no effect

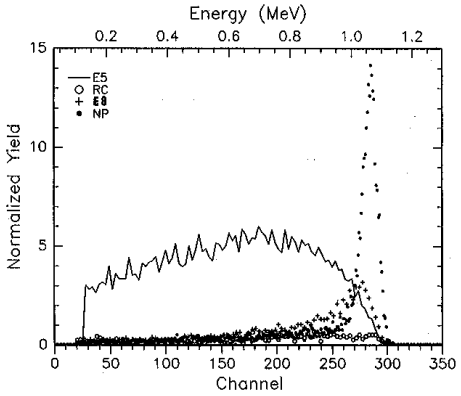

Fig. 9. ERDA spectra for samples altered at acid pH (E5) and neutral pH (E8, RC), compared to the spectrum for nonaltered sample (NP). The respective RBS spectra for these samples are shown in Figs. 6a,b and 7. The large yield peak of the nonaltered sample indicates a surficial H enrichment (probably due to a higher signal/noise ratio and/or surface damage and hydration during polishing) to a depth below the resolution of the technique (~1000 Å). The spectra of E8 and RC indicate very little H penetration. Note that RC may have an anomalously low H concentration; see text for details. Sample E5 shows H penetration, at a constant concentration, over the entire probed depth (~1 μm). These results confirm the strong pH dependence of H incorporation.

on the H concentrations measured at the end of an experiment. This is shown in Fig. 9, where the surficial H concentrations in the altered samples are significantly lower than in the nonaltered sample. A similar observation was made by Petit et al. (1989c), where H concentrations close to the surface decreased as a function of reaction time.

The two samples reacted at neutral pH conditions also show only a shallow enrichment of H. Sample E8, reacted for only 1 h shows a greater amount of H incorporation than sample RC, which was reacted for 24 h. It is possible that RC may have lost H that was originally present and measured by RNRA (see Fig. 3). This may be a consequence of storage in air over a period of 6 years (the RNRA measurements were originally made in 1990). It should be kept in mind, however, that H measurements at the very near surface are susceptible to large errors, due in part to the very near surface having the greatest changes in stoichiometry with respect to the bulk, as well as surface rugosity.

The most important information regarding H penetration is contained in the spectrum of sample E5. Alteration at pH 3.3 for 24 h resulted in the pervasive penetration of H over a depth exceeding the probed thickness, which is on the order of 1 μm. The decrease of the normalized H yield with decreasing energy reflects the dependence of the cross section as a function of the beam energy. The actual H concentration remains constant over the entire probed depth. The relative differences in the depths of H penetration at acid vs. neutral pH conditions is consistent with the RNRA results presented earlier (Fig. 3) which show that H incorporation in the leached/H-enriched zone falls off sharply with increasing pH. In addition, the ERDA results for sample E5 complement the RNRA data shown in Fig. 3 for the sample altered at acid pH. Even though we did not attempt to derive absolute H concentrations from the ERDA spectrum, we can now speculate that the H concentration plateau for acid pH dissolution in Fig. 3 can be extended from 6,000 to 10,000 Å.

3.4. Solution results

Information pertaining to aqueous measurements taken during the dissolution runs of the samples analyzed by RNRA, RBS, and ERDA is given here. In general, data for the samples reacted at 300°C at acid, neutral, and basic pH is limited, especially due to a lack of consistent sampling during the very initial stages ($t < 2$ h) of each of the respective experiments. However, these data have been supplemented by results from Part II that pertain to other albite samples which were dissolved under temperature and pH conditions similar to those in the present study. In Part II, the stoichiometry of the aqueous products (i.e., [Na], [Al], and [Si]) during dissolution was recorded as a function of time. These data complement the information contained in the elemental depth profiles.

With respect to the samples reacted at acid pH in this study, the measured Na and Si release rates were stoichiometric within the error of the analyses. Even though Na leaching depths were not determined for these particular samples, one can compare Na leaching depths determined for samples dissolved at 300°C and acidic pH conditions. For example, at pH 2.2, Na leaching depths were determined to vary from 151 to 1405 Å; at pH 4.0 a Na leaching depth of 245 Å was calculated (see Table 1, Part II; depths based on a linear depletion gradient). The samples reacted at neutral pH also displayed stoichiometric dissolution over the course of the experiments (for $t > 2$ h). Samples from the study in Part II that were dissolved under the same conditions yielded Na leaching depths ranging from ~0 to 249 Å. As was the case at acid and neutral pH conditions, there were insufficient data to calculate precise Na leaching depths for the samples dissolved at basic pH. Nonetheless, intermittent sampling provided evidence for the preferential release of Na over Si. Sodium leaching depths from Part II, based on samples dissolved at 300°C under basic pH conditions, appear to be shallow and not more than a few hundred Å in depth (see Table 1, Part II).

4. DISCUSSION

4.1. Depths of Na Leaching: Comparison of Aqueous and Near-Surface Analytical Measurements

Overall, the Na profiles and spectra determined by RNRA and RBS, respectively, reveal Na leaching to generally occur to much greater depths than determined from the aqueous data in Part II. This discrepancy in leaching depths is not restricted to the results presented in this study. Many studies in the literature have demonstrated preferential leaching in feldspars, to depths ranging up to several thousands of Å at temperatures <50°C, based on diverse surface and near-surface analytical techniques (e.g., SIMS, XPS, ERDA, RNRA, RBS; see numerous references cited in the Introduc-

tion). In contrast, leaching depths based solely on the aqueous products of dissolution are generally more than an order of magnitude less important. The majority of feldspar dissolution studies at 25°C show the formation of leached layers with thicknesses not exceeding ~100–150 Å, as determined by solution analyses (e.g., see Fig. 15, Part II, showing leaching depths as a function of plagioclase composition). An exception to this has been noted for feldspars with a high anorthite content (e.g., labradorite), where extended periods of nonstoichiometric dissolution have resulted in leached layers with much greater thicknesses (see Sjöberg, 1989; Stillings and Brantley, 1995; Schweda and Sjöberg, 1997). The labradorite study by Schweda and Sjöberg (1997) is noteworthy in that their SIMS-determined depths of leaching are in good agreement with leaching depths based on their solution results.

As discussed in detail in Part II, aqueous data lead to leaching depth estimates that are inherently conservative. Perhaps the most important reason for this is due to the fact that solution analyses do not provide information on the shape of the depletion profile, and, therefore, various types of depletion profiles must be assumed in order to calculate depths of leaching. Commonly, leached layers are represented by a near-surface region of complete (100%) depletion, and a step function profile is used to represent the interface between the depleted zone and the unaltered mineral (see, for example, Chou and Wollast, 1984). Alternatively, a linear depletion profile can be used (as in Part II), where the concentration gradient, for example, is based on boundary conditions of 100% depletion at the fluid/solid interface and 0% depletion at the leached layer/unaltered structure interface. Nonetheless, both step function and linear depletion profiles are based on unrealistic gradients and boundary conditions. This necessarily results in an underestimation of leaching depths.

On the other hand, directly-measured profiles using various near-surface analytical tools, such as ion beam and electron spectroscopy techniques, are commonly sigmoidal in shape (e.g., Casey et al., 1988; Hellmann et al., 1990a). In addition to this, these profiles often display long tails in the direction of the unaltered structure, where these tails represent an asymptotic approach to 0% depletion (e.g., XPS results in Hellmann et al., 1990a). This in itself can extend the depth of leaching considerably. It is difficult to ascertain, however, whether these extended tails are always real or not, since they may simply be a function of the decreasing accuracy of these analytical techniques with increasing depths of analysis (for RNRA accuracies, see Dran et al., 1988; Petit et al., 1990a,b).

Another point that is important in comparing solution and ion beam results is that the solution analyses represent the global dissolution behavior of albite. The ion beam profiles and spectra, on the other hand, represent information restricted to specific surfaces ((010) in the present study) and are derived from beam spot areas on the order of 1–3 mm^2 for RNRA and RBS, and up to 20 mm^2 for ERDA. Since no other surfaces were analyzed, we cannot be certain that leaching and H enrichment occur in the same manner on all surfaces, as well as in all relevant crystallographic directions. Nonetheless, Casey et al. (1988) did not note any significant differences in H profiles for (001) and (010) planes in labradorite subjected to dissolution at 25°C under acid pH conditions. This type of result, however, needs to be investigated in the future with respect to albite reacted at 300°C.

A question often raised concerns the presence of structural defects and microtextures that may provide enhanced diffusional pathways (e.g., Balluffi, 1984) for H infiltration and cation release from the structure. This argument has been invoked to explain deep H penetration into crystalline structures, as well as incongruent cation release over extended periods of time. Many studies in the literature have noted that feldspars with high anorthite contents (e.g., oligoclase and labradorite) do not dissolve congruently, even after thousands of hours of dissolution (Sjöberg, 1989; Shotyk and Nesbitt, 1992; Stillings and Brantley, 1995; Schweda and Sjöberg, 1997). This incongruent dissolution behavior has been attributed to enhanced diffusional transport rates along various types of grain and crystallographic boundaries, or alternatively, to differential dissolution rates of exsolved phases (e.g., Eggleton, 1986; Inskeep et al., 1991; Nesbitt et al., 1991; Stillings and Brantley, 1995; Lee and Parsons, 1995).

Even though conclusive proof is not available, it is not likely that the H and Na profiles in the present study are due to enhanced transport rates by structural control. Two primary reasons can be cited: first, the release of elements from albite rapidly becomes congruent during dissolution runs at elevated temperatures, suggesting that pathways of enhanced diffusion are not important; and secondly, RNRA profiles of albite glass (which does not have twin and cleavage planes) are roughly similar to those of crystalline albite (R. Hellmann, unpubl. results).

One other result that is not clear concerns itself with the total amount of Na lost under neutral and basic pH conditions. According to the aqueous results in Part II, minimum depths of Na leaching occur in the neutral pH region. At basic pH, the results were variable, such that in some cases, no preferential leaching of Na was observed, and in others, Na leaching depths up to several hundred Å were determined. This variability precluded the establishment of an unambiguous trend in the neutral to basic pH region, as is discussed in detail in Part II. The RNRA results, on the other hand, show a greater amount of total Na loss at neutral vs. basic pH conditions. Figure 4a,b show that to a depth of approximately 500 Å, the degree of Na loss is roughly the same at neutral and basic pH, but at greater depths, the amount of Na loss at basic pH is insignificant. At present, it is not clear why the solution and near-surface analytical results are not in accord. It is certain, however, that more solution data are needed in order to better constrain the stoichiometric behavior of albite dissolution in the basic pH region.

At present, we are not aware of any studies that have measured Na profiles in feldspars reacted in solutions with pH's ranging from neutral to basic. Thus, we cannot directly compare our Na RNRA results at basic pH. Nonetheless, there appears to be a certain generalized variability in Na RNRA profiles in the literature, as was noted in the discussion above concerning Na depletion at neutral pH (e.g., 100% Na depletion at shallow depths measured after dissolution at neutral pH and 200°C; Petit et al., 1989b). A precursory explanation for the variability in both the aqueous and

RNRA profile results may be related to the inherent high mobility of interstitial cations, such as Na. Even though Na diffusion rates have not been measured directly in the present study, diffusion modeling results (see Part IV) suggest that Na diffusion rates are very rapid, by up to several orders of magnitude greater than rates of H diffusion.

4.2. H/Na Ratios and Ion Exchange

Figure 10 presents H/Na ratios as a function of depth for dissolution at acid, neutral, and basic pH conditions at 300°C. For a given depth, the H/Na ratio is defined as the concentration of incorporated H divided by the concentration of released Na. The amount of released Na at a given depth is calculated from $[Na]_{bulk} - [Na]_{meas}$. The H/Na ratio can be used to quantify the interrelated nature of H infiltration and Na release. The results presented in Fig. 10 show that at acid pH, the ratio of H/Na monotonically increases from ~1.2 at the surface to ~2.3 at a depth of ~2500 Å. At neutral pH the H/Na ratio ranges between ~1.0 and 0.7, and at basic pH the ratio is ~0.4. For dissolution at acid pH, the H/Na ratios are greater than one, indicating that more H is incorporated in the structure than Na is lost. At neutral pH there is a rough equivalency between H uptake and Na loss. At basic pH, the ratio is less than one. This observation may relate to the very limited loss of Na at basic pH conditions (see RNRA profile in Fig. 4a,b) being compensated for by exchange with aqueous species other than H ions. The RBS spectra presented earlier for dissolution in a KOH/H_2O solution (Fig. 8) do not show any significant Na loss, but the presence of K to significant depths is potentially related to the penetration of aqueous species, such that K^+ possibly charge balances lost Na^+. Based on the available data, however, it is still ambiguous as to whether ion exchange reactions occur at basic pH conditions and elevated temperatures.

It is commonly accepted that charged H species in solution are exchanged on a 1:1 charge basis with Na (or other alkali and alkaline earth cations), as has been demonstrated by numerous acid-base titration studies of feldspars (see Garrels and Howard, 1957; Chou and Wollast, 1985; Stillings et al., 1995). If, hypothetically, only ion exchange occurs within altered layers, then the H/Na ratio can be directly used to deduce the nature of the exchange mechanism and species. The following examples illustrate this:

$$H/Na = 3 \quad H_3O^+ \leftrightarrow Na^+ \tag{1}$$

$$H/Na = 1 \quad H^+ \leftrightarrow Na^+ \tag{2}$$

$$H/Na = 1\text{–}3 \quad H^+ \leftrightarrow Na^+ + H_2O_{free} \tag{3}$$

Reactions 1 and 2 represent pure ion exchange mechanisms. Experiments concerning the dissolution of silicate minerals and glasses typically show H/Na values ranging between 1 to 3 (Dran et al., 1988; Petit et al., 1990b). These studies have suggested that H/Na ratios between 1 and 3 are indicative of ion exchange associated with the infiltration of free water molecules (Eqn. 3), or alternatively, ion exchange of hydronium ions (Eqn. 1), followed by the loss of H via condensation reactions. Condensation reactions of silanol groups were first noted in glass dissolution studies (Pederson et al., 1986; Bunker et al., 1988), and have consequently been postulated to occur in a similar manner in crystalline silicates (Casey et al., 1988; Petit et al., 1990a).

Condensation reactions involve the repolymerization of adjacent ≡Si—OH groups as follows: ≡Si—OH + HO—Si≡ → ≡Si—O—Si≡ + H_2O. The net effect of this reaction is the loss of H and O in the structure, accompanied by the production of free water molecules. The ratios of H/Na shown above in Eqns. 1–3 may also be a function of temperature. Dran et al. (1988) suggest that ion exchange reactions are favored at lower temperatures, whereas the pervasive infiltration of water molecules is favored at elevated temperatures. As will be discussed next, the interpretation of H/Na ratios cannot entirely be viewed in the context of ion exchange and water gain or loss, but they must also include the effects of Al preferential leaching and the creation of silanol groups.

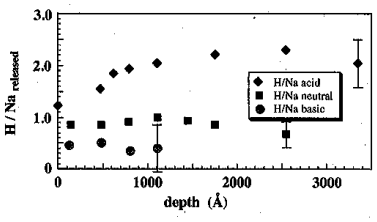

Fig. 10. The ratio of H incorporated to Na released (i.e., Na loss) as a function of pH. The ratios at acid pH indicate that more H is incorporated than Na is released within the leached/H-enriched structure. At neutral pH, H incorporation and Na loss are roughly equal, while at basic pH, the ratios are less than one, possibly indicating Na ion exchange with other aqueous species.

4.3. H/Na Ratios, Ion Exchange, and Aluminum Hydrolysis

The analysis of the H/Na ratios in the present study is not straightforward, mainly due to the premise that dissolution and the creation of leached/H-enriched layers is not simply a function of ion exchange. Thus, it is not possible to differentiate between the various types of H species that infiltrate the structure, based solely on the H/Na ratios. In order to fully understand these ratios, other sinks for H within the structure must be considered.

One very important mechanism for incorporating H into the structure is through the preferential release of Al. As shown in Part II (see Table 1), at 300°C Al is preferentially released under acid and neutral pH conditions (despite the obscuring effects of Al precipitates), as well as under extremely basic pH conditions (pH > 9.5 at 300°C). The preferential release behavior of Al and Si at weak to intermediate basic pH conditions (5.7 < pH < 9.5) is not yet well understood, in that either Al or Si may be preferentially released (to shallow depths, see Part II for a detailed discussion).

The preferential release of tetrahedrally-coordinated Al can be represented by the following equations:

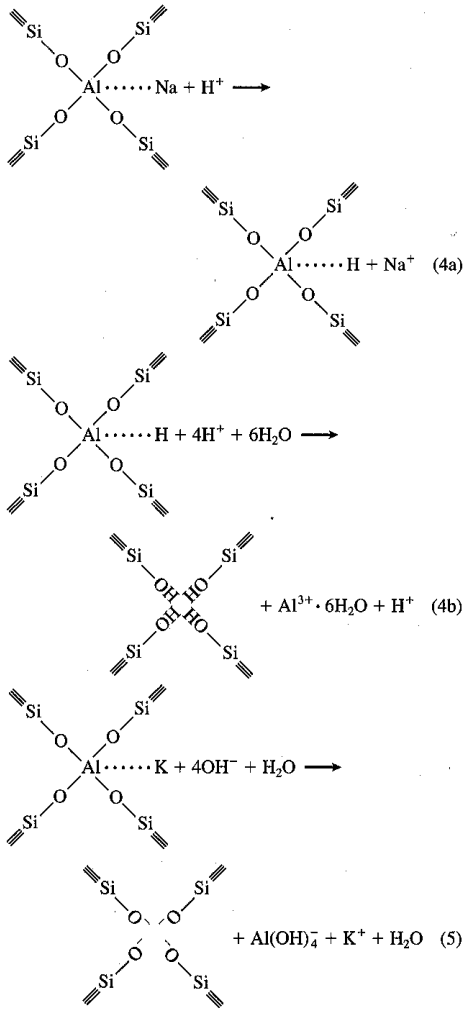

Equation 4a shows the initial ion exchange reaction between Na^+ and H^+ (dotted lines represent purely electrostatic bonding). Equations 4b and 5 portray hydrolysis reactions that lead to the creation of silanol groups and the release of Al at acidic and basic pH conditions, respectively. Equation 5 presupposes dissolution in a KOH/H_2O solution and an initial ion exchange reaction between Na^+ and K^+ (the identity of the charge-balancing interstitial cation has no effect on the hydrolysis reaction as shown). The important point in Eqn. 5 is the creation of $\equiv Si—O^-$ groups. The negative $\equiv Si—O^-$ groups may be charge compensated by interstitial K^+ ions. This represents an alternative explanation (vs. Na^+ and K^+ ion exchange) for the potential presence of K to significant depths in the leached structure (see RBS spectrum E17, Fig. 8).

The above reactions do not show the various elementary steps which are a part of the overall hydrolysis processes. The hydrolysis reactions include the presence of water, in accord with recent ab initio calculations (Xiao and Lasaga, 1994, 1996). At acid pH, these calculations show that there is no energetic difference between hydrolysis involving H^+ and H_2O vs. H_3O^+. As shown above, the free Al groups possess an overall charge of +3 at acid and −1 at basic pH conditions, respectively. The speciation and charge of each free Al group is of course dependent on pH. The exact mechanism for the transformation of Al from tetrahedral coordination within the structure to sixfold coordination in solution is not well-understood (see Casey et al., 1989b), especially with respect to whether this occurs in situ at the sites of hydrolysis, during diffusion within the leached/H-enriched layer, or at the fluid/solid interface.

In regard to the incorporation of H into the structure, it is the creation of silanol groups which is of primary interest. Under acidic conditions, the hydrolysis of bridging oxygen bonds in each $\equiv Si—O—Al\equiv$ linkage results in the creation of a silanol group, shown as $\equiv Si—OH$ (Eqn. 4b). On the other hand, under basic pH conditions, each silanol group which is created instantly deprotonates, resulting in the formation of a negatively-charged $\equiv Si—O^-$ group (Eqn. 5). In both cases, the proportion of $\equiv Si—OH$ to $\equiv Si—O^-$ groups is a function of the pH and the acid-base constants of $\equiv Si—OH$ at the temperature of interest. At 25°C, surface $\equiv Si—OH$ has the following acid/base constants: $pK_{a1} \approx -2.0$ and $pK_{a2} \approx 6.6$ (constants based on amorphous silica, pK_{a2} value averaged from Schindler and Kamber, 1968; and Sigg, 1973). At 25°C, therefore, $\equiv Si—OH$ groups start to predominate at pH < 6.6 and $\equiv Si—O^-$ groups predominate at pH > 6.6. At this point, the reader should note that it is implicitly being assumed that the protonation/deprotonation behavior of $\equiv Si—OH$ groups within the leached zone is the same as at the surface.

Due to a lack of thermodynamic data concerning $\equiv Si—OH$ at elevated temperatures, the exact calculation of pK_{a1} and pK_{a2} at 300°C is not attempted. At present, studies pertaining to silica surface chemistry at elevated temperatures are restricted to $T < 100$°C (Brady, 1992; and references therein). However, it is generally accepted that pK_a values for most metal-OH groups decrease with increasing temperature up to ~200°C. At temperatures > 200°C, it is not clear whether pK_a values continue to decrease, become constant, or actually increase (for more details, see Machesky, 1990; Machesky and Jacobs, 1991; Schoonen, 1994; Machesky et al., 1994; see also discussion in Part II).

Despite the lack of reliable estimates for pK_{a1} and pK_{a2} for $\equiv Si—OH$ groups at temperatures above 100°C, we assume that at 300°C $\equiv Si—OH$ groups predominate at pH 3.4, and that $\equiv Si—O^-$ groups predominate at pH 8.6. In the neutral pH range (pH = 5.7), $\equiv Si—OH$ and $\equiv Si—O^-$ groups most probably coexist, in an unknown proportion. The important point is that the removal of a tetrahedrally-coordinated Al results in the maximum incorporation of 4 H atoms into 4 silanol groups (for a net gain of 3 H atoms-see Eqn. 4b) under pH conditions where $\equiv Si—OH$ groups

predominate. As the pH of the solution becomes more basic, the number of H atoms incorporated decreases, concomitant with a decrease in the ratio $\equiv Si-OH/\equiv Si-O^-$. Therefore, the release of Al under basic pH conditions (Eqn. 5), where $\equiv Si-O^-$ groups predominate, would not result in the incorporation of H into silanol groups within the leached structure.

From the above discussion, it now becomes apparent that two processes are primarily responsible for the direct incorporation of H into the structure: ion exchange and the preferential release of Al. In addition, the infiltration of water molecules can also be considered to be a process which leads to an increase in the H-content of the structure; this is discussed further on. On the other hand, H loss from the structure can also occur, mainly via condensation reactions of adjacent $\equiv Si-OH$ groups. Starting with four adjacent silanol groups resulting from the preferential release of one Al atom (right hand side of Eqn. 4b), a condensation reaction can be schematically represented as follows:

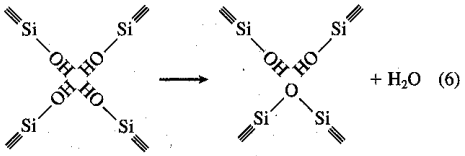

$+ H_2O$ (6)

Na and H profiles, which are not perfectly anticorrelated, have been used as evidence for restructuring (repolymerization) via condensation reactions. In a study of silicate glass and mineral dissolution, Petit et al. (1990a) measured a sharp decrease in H concentrations close to the surface, which was not anticorrelated with the corresponding Na profile. They attributed this mismatch in the profiles as possible evidence for restructuring via condensation reactions (see Fig. 6, Petit et al., 1990a). In the present study, there is also a mismatch between the Na and H profiles, particularly for the case at acid pH (see Figs. 3 and 4a). However, at acid pH, the H profile does not show any sudden drop close to the surface, which might be expected if recondensation reactions were important. The H profiles at neutral and basic pH also do not show behavior that could be ascribed to recondensation. Nonetheless, as will be shown later on, H profiles corrected for Na ion exchange provide evidence for recondensation reactions close to the surface that is not readily apparent in the profiles representing overall H concentrations.

4.4. The pH-Dependency of Hydrogen Incorporation

According to the results from the present study, there is a strong inverse relationship between the pH conditions of dissolution and the amount of H incorporated into the structure (RNRA profiles in Fig. 3; ERDA spectra in Fig. 9; H/Na ratios in Fig. 10). This type of pH-dependency in feldspar leached/H-enriched layers has also been observed in other studies (see Casey et al., 1988, 1989a; Schweda and Sjöberg, 1997). These results are also consistent with results from silicate glass dissolution studies carried out at pH 1–12 by Bunker et al. (1983). Of particular note in the present study, as well as those cited above, is the fact that there is no difference between the H profiles of feldspars reacted at basic pH and nonreacted, reference samples.

According to Petit and coworkers (Petit et al., 1989b, 1990b), the decrease in the amount and depth of H penetration with increasing pH reflects both a decrease in the proton activity in solution (which serves to diminish ion exchange and decrease the rate of H diffusion) and an increased degree of network hydrolysis under basic pH conditions, such that significant leached layers do not develop at basic pH conditions. Based on dissolution studies of labradorite feldspars, Casey et al. (1989a) attribute the lack of H penetration at basic pH to a dissolution process that proceeds via a different mechanism from that at acid pH. They hypothesize that the adsorption of hydroxyl ions at the surface does not proceed via an exchange of alkalis, and therefore no leached layers are formed. For this reason, they proposed a mechanism where the surface activated complex contains a framework constituent (Al or Si), as well as a charge-compensating ion, such as Na or Ca (Casey et al., 1989a).

However, the question that should be raised is whether the H profiles measured by various near-surface analytical techniques are truly representative of measuring how much H participates in the dissolution process. It seems much more likely that the H signal is a measure of how much H infiltrates the structure and is then subsequently incorporated by chemical bonding to the structure. This distinction is important in that it implies that at basic pH, for instance, hydroxyls and water molecules may participate during hydrolysis reactions within a leached/H-enriched region, but they are not chemically incorporated into the leached structure. The XPS study by Hellmann et al. (1990a) shows the presence of Ba^{2+} to depths of 500 Å when albite is dissolved in a $Ba(OH)_2/H_2O$ solution at 225°C. The RBS spectra in the present study show the possible enrichment of K to significant depths as a consequence of dissolution in KOH/H_2O solutions. The possible incorporation of Ba is also shown by the RBS results shown in Fig. 8. Nonetheless, evidence in the form of near-surface profiles for all preferentially leached and infiltrating species is needed to confirm this point, however.

In the following paragraphs, we summarize several alternative explanations for the observed pH-dependency of H incorporation, based on ion exchange and the preferential release of Al from the structure.

The diffusion of H into the structure is dependent on the H^+ gradient between the solution and the structure. This chemical gradient is, of course, dependent on the pH of the solution, such that H^+ permeation will be most rapid and pronounced at acid pH conditions (in accord with Petit et al., 1989b, 1990b).

The $H^+ \leftrightarrow Na^+$ exchange reaction predominates at acid pH. At basic pH, there is possible evidence for a limited degree of ion exchange between cations in the solution and Na in the structure (see evidence above). This ion exchange is much less significant than the ion exchange that occurs at acid pH conditions. One possible reason for this is that cation exchange is hindered by the larger sizes of these cations in comparison to H ions. This is probably the main reason why the amount of H infiltration at acid pH conditions is far more significant than K infiltration is at basic pH conditions, for example (or with respect to any other positive cations present).

The preferential release of Al from the structure and H incorporation are related, due to the fact that the release of

Al leads to the concomitant formation of silanol groups. As shown in Eqn. 4b, for each Al removed, a maximum of 4 H are incorporated into silanol groups at acid pH, whereas at basic pH, no H is incorporated (Eqn. 5). The degree of H incorporation is dependent on the proportion of ≡Si—OH/≡Si—O^- groups, which in turn, is a function of pH and temperature.

As shown in Part II (and references therein), the depth of Al leaching decreases as pH increases from acid to neutral pH. In the neutral to basic pH range, Al leaching depths are variable. The trend of decreasing H incorporation with increasing pH in the acid to neutral pH range can, therefore, be partly attributed to the concomitant decrease in the overall degree of preferential Al release.

4.5. Hydrogen Associated with Aluminum Hydrolysis and Leaching

The respective importance of protons, hydronium ions, hydroxyl ions, and molecular water during the dissolution process is still not well understood. As stated by Casey et al. (1988), the relation between H incorporation and overall dissolution rates is unclear. In this section, the H and Na RNRA data are used to quantify the various sinks for H in the leached/H-enriched structure. The first step is a calculation of how much H is involved with ion exchange and the hydrolysis and preferential leaching of Al in the structure.

The starting point is a determination of the excess H that is left over after the Na^+-H^+ ion exchange process. For the purposes of these mass balance calculations, the exchange reaction is assumed to involve only H^+ and not H_3O^+. Excess H is simply a measure of H in the structure that is chemically bonded or physically sorbed to sites not associated with Na exchange sites. Excess H is defined as

$$[H]_{excess} = [H]_{meas} - [Na]_{released} \quad (7)$$

$$[H]_{excess} = [H]_{meas} - ([Na]_{bulk} - [Na]_{meas}) \quad (8)$$

The excess H can be used as a constraint on how much H is involved in the hydrolysis of ≡Si—O—Al≡ bonds, as well as that associated with chemically unbound H present within the leached/H-enriched zone (such as free water molecules).

Figure 11 shows H excess profiles. The relative positions of the acid, neutral, and basic pH curves is a function of both the degree of Al preferential leaching, as well as the speciation of ≡Si—OH groups within the leached/H-enriched zone. As an example, in comparing the excess H present after dissolution at acid and neutral pH, the difference in H concentrations reflects the greater degree of preferential release of Al at acid pH, as well as a higher ratio of ≡Si—OH/≡Si—O^- groups in the leached/H-enriched layer. The position of the excess H curve at basic pH most likely reflects the predominance of ≡Si—O^- groups in the leached/H-enriched layer. It may, of course, also be due to a lack of Al preferential leaching during the dissolution run. Unfortunately, this cannot be verified due to the paucity of solution data collected during the initial stages of the experiment.

Perhaps the most interesting aspect of these results is the sharp drop in the acid pH excess H curve near the immediate surface (Fig. 11, depth <700 Å). As mentioned earlier (Experimental Methods), H measurements close to the surface (depths <250 Å) can be subject to large errors, and, therefore, the sharp drop may simply be an artifact. On the other hand, if the trend is real, it may be indicative of a distinct decrease in H associated with ≡Si—OH sites in the leached/H-enriched structure. One of the most likely reasons for this is the condensation of adjacent ≡Si—OH groups, which results in the loss of H and O from the structure (schematically represented by Eqn. 6). It is interesting to speculate that the probability for condensation reactions to occur may be a function of the density of adjacent ≡Si—OH groups. Given that ≡Si—OH groups are more prevalent at acid pH, where the preferential release of Al is more pronounced, then it is likely that restructuring of the near-surface via condensation is favored to occur at acid pH dissolution conditions.

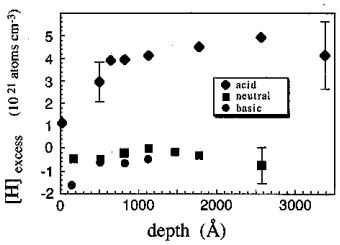

Fig. 11. Excess H incorporated as a function of pH. The excess H is the amount of H that does not participate in ion exchange with Na, therefore, it is a measure of H that is either incorporated in ≡Si—OH and ≡Al—OH groups, or is present as a free H species (e.g., water). The decrease in the H/Na ratio at depths <700 Å at acid pH may be indicative of recondensation reactions of ≡Si—OH groups, resulting in the loss of H and O (see text for details).

Additional evidence for recondensation reactions is possibly revealed by decreases in O in the leached/H-enriched region. Depletion of O from the structure would be expected as a consequence of condensation of ≡Si—OH groups and the creation of free H_2O (Eqn. 6). A quantitative interpretation of the O concentrations in the RBS spectra in Figs. 6–8 is not possible. However, a significant depletion in O concentrations was observed by XPS of hydrothermally altered albite by Hellmann et al. (1990a). In a SIMS study by Schweda and Sjöberg (1997), O/Si was measured in labradorite altered under acid pH conditions. The O/Si decreased from 3.3 in the bulk structure to 2.0–2.5 in the leached structure. This is also possible evidence for recondensation reactions.

4.6. Permeation of Molecular Water

In the previous section, the amount of incorporated H, corrected for Na exchange, was calculated. This excess H includes H bound to ≡Si—OH groups, as well as unbound H. The purpose of this section is to determine the amount of unbound H present in the leached/H-enriched structure (for dissolution under acid pH conditions). It can be assumed, but not proven, that the majority of unbound H is in

the form of physisorbed or H-bonded water. The relationship below is used to define free H not chemically bonded to the structure. The first term on the right defines [H] corrected for ion exchange (see Eqns. 7, 8), and the second term on the right is equal to [H] associated with silanol groups

$$[H]_{free} = [H]_{excess} - [H]_{\equiv Si-OH} \quad (9)$$

Equation 9 can be decomposed and re-expressed as follows:

$$[H]_{free} = [H]_{meas} - [Na]_{released} - 3[Al]_{released} \quad (10a)$$

$$[H]_{free} = [H]_{meas} - [Na]_{released} - n[Na]_{released} \quad (10b)$$

The second and third terms on the right-hand side of Eqn. 10a show that H incorporation into the H-enriched zone occurs on a 1:1 basis with Na (ion exchange) and on a 3:1 basis with Al (hydrolysis and creation of silanol groups- see Eqn. 4b). Equation 10b results from replacing the unknown quantity [Al] by n[Na]. Note that the relative degree of Na to Al preferential leaching is given by the value of n. If Na and Al release are stoichiometric, $n = 3$. It follows that $0 < n < 3$ for all intermediate cases where the moles of Al leached are inferior to that of Na.

To illustrate the use of the approach described above, we present a series of simple mass balance calculations, based on the RNRA results at acid pH. Similar calculations at neutral and basic pH were not carried out, mainly due to the dramatically lower levels of H present in their respective H-enriched regions. At a depth of 1100 Å (data for acid pH shown in Figs. 3 and 4b), for example, knowledge of [H] and $[Na]_{released}$ permits the calculation of the excess H, based on Eqns. 7 and 8 (concentrations $\times 10^{21}$ atoms cm^{-3}):

$$[H]_{meas} - [Na]_{released} = [H]_{excess} \quad (11)$$

$$8.06 - 3.90 = 4.16$$

In the following calculation, use is made of the mass balance approach given in Eqn. 10a,b. To calculate $[H]_{free}$, $[H]_{excess}$ is decreased by [Na] that corresponds to an Al/Na release ratio of ⅓. This nonstoichiometric release, which was arbitrarily chosen, corresponds to $n = 1$ in Eqn. 10b. Thus, we can write

$$[H]_{free} = [H]_{excess} - 1x[Na]_{released} \quad (12a)$$

$$0.26 = 4.16 - 3.90$$

$$[H]_{free} = [H]_{excess} - \tfrac{1}{3}[Al] \quad (12b)$$

As can be seen by the result in Eqn. 12a,b, free H represents only 3% of the total H incorporated (0.26/8.06 for $n = 1$). In the same manner as above (Eqn. 12a), greater degrees of Al loss can be formulated in terms of $n = 2$ and 3. For $n = 2$, there would be no free H. The conclusion that can be drawn from these results is that the concentration of free H species (probably in the form of molecular water) is probably negligible within the leached/H-enriched structure. This same conclusion was reached by Schweda and Sjöberg (1997), based on measured O/Si ratios that were significantly lower in acid leached vs. unaltered labradorites.

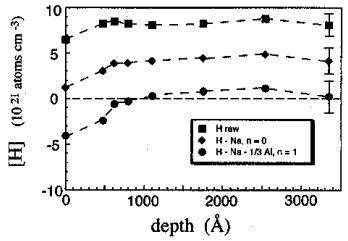

Fig. 12. Hydrogen concentrations as a function of depth for dissolution at acid pH. The upper most curve shows $[H]_{meas.}$ (as in Fig. 3). Subsequent curves show H concentrations corrected for Na ion exchange, as well as increasing amounts of Al preferential leaching, denoted by values of $n = 0$ and 1, respectively (see text for details). The lowest most curve shows that little if no free H species are present within the leached/H-enriched zone.

Figure 12 shows the concentrations of free H after dissolution at pH 3.4 to a depth of 3500 Å (the depth limit of the RNRA data), based on the calculations shown above. Starting from the top of the figure, the first curve represents the concentration of raw H, as directly measured by RNRA; this is the same curve as presented in Fig. 3. The second curve represents excess H (i.e., [H] corrected only for ion exchange with Na and no leaching of Al; Eqns. 7, 8); this curve is the same as the $[H]_{excess}$ curve at acid pH in Fig. 11. The third curve represents the concentration of free H, based on Al leaching that is quantitatively only one third that of Na leaching (i.e., $n = 1$; Eqns. 10b, 12a,b). As can be readily seen in the figure, the amount of free H is negligible under these conditions at depths > 1000 Å. At depths < 1000 Å, there is an apparent H deficit, which is possibly indicative of H loss due to recondensation reactions.

Based on the aqueous results presented in Part II, it is difficult to exactly estimate the relative degrees of Na and Al leaching. Based on XPS profiles presented in Hellmann et al. (1990a), the degrees of Al and Na leaching are roughly equivalent for dissolution at 225°C and pH 2.5 (similar results for Ca/Al are shown in Schweda and Sjöberg, 1997). If it is assumed that the relative degrees of Na and Al preferential leaching are roughly equivalent for the conditions of dissolution in the present study (i.e., $n \approx 3$), then the amount of free H in the leached/H-enriched structure would be negative over the entire depth of analysis (curves for $n = 2$, 3 not shown in Fig. 12). This discrepancy in overall free H may point to an overall deficit in the predicted H uptake throughout the leached/H-enriched zone, since the amount of free H is negligible, even for the case when Al leaching is just one third that of Na leaching ($n = 1$). This is additional, albeit indirect evidence for recondensation reactions occurring at even greater depths than previously discussed.

It is interesting to note that in two studies of glass dissolution (Dobos, 1971; Baucke, 1974), it was postulated that protons diffuse ahead of free water into the structure, and that only the very outermost part of the leached zone contained free water. Infrared spectroscopy (IR) is often used to detect and differentiate H species in reacted minerals and glasses, although the information obtained is not depth-spe-

cific. In an infrared spectroscopy study by Behrens (1994), the spectra showed an absence of molecular water in natural plagioclases. For the case of H feldspars (prepared by Na-H ion exchange), this study showed that H is primarily associated with hydroxyl groups suggesting that H species react at bridging oxygen sites, thereby leading to the formation of ≡Si—OH and ≡Al—OH groups. Casey et al. (1988) present IR results based on a 10,000 Å thick altered layer created by alteration of labradorite at acid pH conditions. By far the largest absorbance peak was at 3500 cm^{-1}; this peak was assigned to bound hydroxyl groups (X—OH) and hydrogen bonded water. Their results, however, did not allow for a quantitative interpretation of the IR spectra.

The strong nature of H bonds within a leached/H-enriched glass structure was demonstrated by Petit et al. (1990a), who showed that the degree of H loss from the H-enriched zone was negligible upon heating, even up to temperatures of 400°C. This general nonmobility of H implies that H measured by RNRA is chemically bound to the leached/H-enriched structure. However, the results in the present study concerning sample RC suggest that H diffusion towards the surface over long periods of time may decrease incorporated H levels.

5. CONCLUSIONS

The main emphasis of the present study is a better understanding of the formation of leached layers at elevated temperatures due to the preferential loss of Na and Al from the albite structure. The formation of these leached layers is related to the concomitant incorporation of H into the leached layers. Below we summarize the main conclusions regarding the pH-dependence of H incorporation and Na and Al loss, as well as the incorporation of free H species (e.g., molecular water) into the leached/H-enriched structure.

The experimental results show that dissolution at elevated temperatures (i.e., 300°C) and under acid to neutral pH conditions results in the pervasive infiltration and incorporation of H into the structure, resulting in a zone of H enrichment that extends many thousands of Å into the structure. This extensive H enrichment is evidenced by experimentally measured H concentration plateaus at acid pH conditions that extend to depths beyond the analytical limits of the RNRA (>6000 Å) and ERDA (>10,000 Å) measurements in the present study. Even though there is no experimental evidence, it is assumed that these flat H concentration profiles become sigmoidal at some unknown depth as the H concentrations tend toward zero. This type of behavior, characterized by a saturated H plateau followed by a steep drop in concentration (i.e., a diffusion front), has been observed in naturally hydrated obsidian (Lee et al., 1974). This may point to more than one H diffusion and/or binding mechanism during the dissolution and hydration process (Lee et al., 1974; Ericson et al., 1974).

The Na RNRA profiles show that the loss of Na from the structure is also very significant under acid and neutral pH conditions of dissolution. The measured Na profiles are characterized by extensive depletion plateaus that extend beyond the range of the RNRA analyses (~4000 Å). The qualitative nature of the RBS results only allows for a confirmation of a leached zone at acid pH conditions, to depths of ~20,000 Å. Supporting evidence suggests Na depletion occurs to similar depths. It is important to note that the depths of Na depletion determined from aqueous dissolution data (e.g., Part II) are significantly shallower than those determined directly by the near-surface analytical techniques employed in this study.

Under basic pH conditions, the measured H RNRA profile is indistinguishable from that of the unreacted reference sample. The Na RNRA profile at basic pH reveals that Na depletion is relatively insignificant, occurring to a depth of several hundred Å. It is noteworthy that the amount of Na loss is roughly equivalent to the loss recorded at neutral pH at the very near surface (depth <500 Å). Minor Na^+ loss at basic pH may be compensated by ion exchange with K^+, when dissolution occurs in a KOH/H_2O solution. Possible evidence for this is due to the presence of K in RBS spectra over the entire probed thickness (≈10,000 Å) in samples run in KOH/H_2O solutions. However, the RBS data in this study do not constitute direct evidence that ion exchange at basic pH conditions takes place; only directly measured Na and K depth profiles can prove or disprove this point. Nonetheless, even if ion exchange at basic pH conditions occurs, the $K^+ \leftrightarrow Na^+$ ion exchange reaction, for example, would be much more limited than the H^+ (or H_3O^+) $\leftrightarrow Na^+$ ion exchange reaction at acid pH. This argument is based on size considerations of the aqueous cations that are potentially exchanged with Na^+; the greater the size, the less favorable the exchange reaction.

The amount of H incorporation in the leached/H-enriched structure is a strong function of the pH and temperature conditions of dissolution. Likewise, the amount of Na loss follows approximately the same trend as the H concentration profiles: acid pH > neutral pH > basic pH; high T loss ≫ low T loss. An important conclusion, therefore, is that the composition of the leached/H-enriched layers is a function of pH, and the depth is a function of temperature. One of the most important reasons for this pH-dependency is due to the ion exchange reaction between H^+ (or H_3O^+) and Na^+. The rate of H^+ (or H_3O^+) and Na^+ ion-exchange is a function of their respective concentration gradients which, in turn, determine the rate of inward diffusion of H species and the outward diffusion rate of Na ions. Hydrogen incorporation is also a function of the speciation of ≡Si—OH and ≡Al—OH groups within the leached/H-enriched zone, which are created as a result of Al preferential release. With increasing pH, deprotonation reactions of ≡Si—OH and ≡Al—OH groups serve to decrease the amount of H associated with these groups within the leached/H-enriched structure. Deprotonation reactions resulting in the formation of ≡Si—O^- and ≡Al—O^- groups may provide electrostatic adsorption sites for positive aqueous cations, such as K^+. Directly measured depth profiles of all cations in the leached zone would be a necessary prerequisite for proving this point, however.

At basic pH conditions, the possible presence of K and Ba within leached zones is the basis for speculating that aqueous species are able to penetrate the structure to depths corresponding to that of preferential leaching (i.e., at least several hundreds of Å). For example, H in the form of OH^- ions, with or without the presence of H_2O, most probably permeates the leached zone, since OH^- is necessary in

framework bond hydrolysis reactions at basic pH conditions (Xiao and Lasaga, 1996) that result in the preferential leaching of Al (only at very elevated basic pH conditions). Since $\equiv Si-O^-$ and $\equiv Al-O^-$ groups predominate at basic pH conditions, any H present during the hydrolysis reactions will not remain chemically bound to the leached structure. For this reason a thick H-enriched zone is not created at basic pH conditions. This points out a very important but subtle difference between H permeation and H retention; the latter is what is actually measured by near-surface H sensitive analytical techniques, such as RNRA and ERDA.

Even though the degree of H incorporation and Na retention are inversely related as a function of pH, the experimentally measured H and Na concentrations are not perfectly anticorrelated. There are several reasons for this, including the fact that H species participate in more than just ion exchange reactions, but also in framework bond hydrolysis reactions. In addition, it is possible that H is lost from the structure via recondensation reactions that occur in the outermost part of the leached zone (see acid pH results; Fig. 11). The calculated overall H deficit may even point to pervasive recondensation reactions within the leached/H-enriched zone.

The H to Na release ratios range between 0.7 and 2.3 at acid and neutral pH. Since ion exchange reactions do not exclusively determine this ratio, it is not possible to differentiate between H^+ and H_3O^+ in the overall dissolution process. However, simple mass balance/charge equivalency calculations, involving H incorporation, Na loss, and Al preferential leaching, show that very little if any free H species (i.e., H_2O) are retained in the leached/H-enriched structure after dissolution under acid pH conditions. Even less free H is bound to the structure after dissolution at neutral and basic pH conditions. It is important to note, however, that these conclusions on the lack of free water in the altered/H-enriched structure need to be verified by direct measurements, such as by IR techniques.

The maximum concentration of H that can be incorporated into the leached/H-enriched near-surface structure has a probable maximum limit, on the order of $\sim 1 \times 10^{22}$ atoms/cm^3. This result, based on alteration in acid pH solutions, appears to hold for both albite and labradorite, at both low and high temperatures. It is interesting to note that temperature doesn't seem to influence the concentration of H close to the surface (given long enough reaction time), rather it influences the depth of permeation. This maximum attainable concentration of H suggests that altered near-surface structures in feldspars have a definite crystallographic H-saturation limit.

The influence of crystallographic structure, such as twin boundaries or cleavage planes, is a potentially important factor in interpreting RNRA profiles, as well as the mechanisms of dissolution. Since albite feldspars dissolve congruently, enhanced diffusional transport along crystallographic boundaries is probably not important. Nonetheless, direct experimental evidence confirming this is still lacking. Definitive experiments and measurements to solve this question should be an avenue of promising future research. In addition to this, future experiments should also investigate whether H penetration and preferential leaching are the same in all crystallographic directions.

A final comment should be made in regard to the suitability of RNRA, ERDA, and RBS for near-surface measurements of hydrothermally altered feldspars. The RNRA technique is probably still one of the most accurate and powerful available for the determination of H and Na profiles. Its main disadvantage is its high cost and time-consuming nature. On the other hand, based on the results in this study, RBS is not particularly suited for the quantitative measure of preferential leaching in feldspars. One of the main problems is the overlap of the Al and Si edges, which makes the discrimination of these key elements very difficult when preferential leaching is very deep. Finally, the grazing nature of ERDA ion beam interactions with sample surfaces limits this technique to perfectly flat sample surfaces. Rugose surfaces, as was the case in this study, do not lend themselves to quantitative H measurement. Future studies of this kind may well warrant study with other ion beam techniques, such as SIMS.

Acknowledgments—The first author thanks C. Clerc and F. Garrido (C.S.N.S.M., Orsay) for their time and expertise in obtaining the RBS and ERDA spectra for the second set of samples. The interpretations and conclusions drawn from these spectra remain the sole responsibility of the first author. We also thank our colleagues at the INFN accelerators at Padova for their technical assistance. The first author is indebted to the late Professor David A. Crerar of Princeton University for the 18 month loan of one of the flow systems. This paper is dedicated to his memory. The first set of samples were altered in dissolution experiments conducted at the geochemistry laboratory in Toulouse. In Toulouse, the following people's advice or assistance was appreciated: G. Berger, J.-L. Dandurand, M. Gugeon, C. Lurde, C. Monnin, B. Reynier, and J. Schott. In addition, we thank Societé Bioland for the use of their ICP. Useful discussions with L. Sjöberg and P. Schweda are acknowledged. Lennart Sjöberg unexpectedly passed away in February, 1996. In collaboration with Bob Berner of Yale University, he was among the early researchers to apply surface spectroscopic techniques to mineral weathering. For those who knew him, we will miss his warmth and sense of humor. Reviews by S. Brantley, P. Brady, and an anonymous reviewer much improved the presentation of this study. This article is contribution no. 69 in the C.N.R.S.-DBT II program, "Fluides dans la Croûte."

Editorial handling: J. D. Rimstidt

REFERENCES

Amsel G. and Lanford W. A. (1984) Nuclear reaction techniques in materials analysis. *Ann. Rev. Nucl. Part. Sci.* **34,** 435–460.

Balluffi R. W. (1984) Grain boundary diffusion mechanisms in metals. In *Diffusion in Crystalline Solids* (ed. G. E. Murch and A. S. Nowick), pp. 319–377. Acad. Press.

Barbour J. C. and Doyle B. L. (1995) Elastic recoil detection: ERD (or Forward Recoil Spectrometry: FRES). In *Handbook of Modern Ion Beam Analysis* (ed. J. R. Tesmer et al.), pp. 83–138. Materials Res. Soc.

Baucke F. G. K. (1974) Investigation of surface layers, formed on glass electrode membranes in aqueous solutions, by means of an ion sputtering method. *J. Non-Cryst. Solids* **14,** 13–31.

Behrens H. (1994) Structural, kinetic, and thermodynamic properties of hydrogen in feldspars. In *Kinetics of Cation Ordering* (ed. A. Putnis), pp. 1–7. Cambridge Univ.

Berner R. A. and Holdren G. R., Jr. (1979) Mechanism of feldspar weathering-II. Observations of feldspars from soils. *Geochim. Cosmochim. Acta* **43,** 1173–1186.

Brady P. V. (1992) Silica surface chemistry at elevated temperatures. *Geochim. Cosmochim. Acta* **56,** 2941–2946.

Bunker B. C., Arnold G. W., Beauchamp E. K., and Day D. E. (1983) Mechanisms for alkali leaching in mixed-Na-K silicate glasses. *J. Non-Cryst. Solids* **58,** 323–332.

Bunker B. C., Tallant D. R., Headley T. J., Turner G. L., and Kirk-

patrick R. J. (1988) The structure of leached sodium silicate glass. *Phys. Chem. Glasses* **29,** 106–120.

Casey W. H., Westrich H. R., and Arnold G. W. (1988) Surface chemistry of labradorite feldspar reacted with aqueous solutions at pH = 2, 3, and 12. *Geochim. Cosmochim. Acta* **52,** 2795–2807.

Casey W. H., Westrich H. R., Arnold G. W., and Banfield J. F. (1989a) The surface chemistry of dissolving labradorite feldspar. *Geochim. Cosmochim. Acta* **53,** 821–832.

Casey W. H., Westrich H. R., Massis T., Banfield J., and Arnold G. W. (1989b) The surface of labradorite feldspar after acid hydrolysis. *Chem. Geol.* **78,** 205–218.

Cherniak D. J. and Lanford W. A. (1992) Nuclear reaction analysis. In *Encyclopedia of Materials Characterization* (ed. C. R. Brudle et al.), pp. 680–694. Butterworth-Heinemann.

Chou L. and Wollast R. (1984) Study of the weathering of albite at room temperature and pressure with a fluidized bed reactor. *Geochim. Cosmochim. Acta* **48,** 2205–2217.

Chou L. and Wollast R. (1985) Steady-state kinetics and dissolution mechanisms of albite. *Amer. J. Sci.* **285,** 963–993.

Chu W. K., Mayer G. W., and Nicolet M. A. (1978) *Backscattering Spectrometry.* Acad. Press.

Deer W. A., Howie R. A., and Zussman J. (1978) *An Introduction to the Rock Forming Minerals.* Longman.

Della Mea G., Dran J.-C., Petit J.-C., Bezzon G., and Rossi-Alvarez C. (1983) The use of ion beam techniques for studying the leaching properties of lead implanted silicates. *Nucl. Instrum. Meth. Phys. Res.* **218,** 493–499.

Dobos, S. (1971) Strukturumwandlungen des Silikatnetzwerkes im Laufe der Ausbildung der Oberflächenschicht bei natriumhaltigen Gläsern. *Acta Chim. Acad. Sci. Hung.* **69,** 43–48.

Dran J.-C., Della Mea G., Paccagnella A., Petit J.-C., and Trotignon L. (1988) The aqueous dissolution of alkali silicate glasses: Reappraisal of mechanisms by H and Na depth profiling with high energy ion beams. *Phys. Chem. Glasses* **29,** 249–255.

Eggleton R. A. (1986) The relation between crystal structure and silicate weathering rates. In *Rates of Chemical Weathering of Rocks and Minerals* (ed. S. M. Coleman and D. P. Dethier), pp. 21–40. Acad. Press.

Ericson J. E., MacKenzie, J. D., and Berger, R. (1974) In *Advances in Obsidian Glass Studies: Archaeological and Geochemical Perspectives* (ed. R. E. Taylor), pp. XX–XX. Noyes Press.

Garrels R. M. and Howard P. (1957) Reactions of feldspar and mica with water at low temperature and pressure. *Proc. 6th Natl. Conf. Clays Clay Minerals,* 68–88.

Harlow G. E. and Brown G. E., Jr. (1980) Low albite: An X-ray and neutron diffraction study. *Amer. Mineral.* **65,** 986–995.

Hellmann R. (1994) The albite-water system: Part I. The kinetics of dissolution as a function of pH at 100, 200, and 300°C. *Geochim. Cosmochim. Acta* **58,** 595–611.

Hellmann R. (1995) The albite-water system: Part II. The time-evolution of the stoichiometry of dissolution as a function of pH at 100, 200 and 300°C. *Geochim. Cosmochim. Acta* **59,** 1669–1697.

Hellmann R. (1997) The albite-water system: Part IV. Diffusion modeling of leached and hydrogen-enriched layers. *Geochim. Cosmochim. Acta* **61,** 1595–1611.

Hellmann R., Eggleston C. M., Hochella M. F., Jr., and Crerar D. A. (1990a) The formation of leached layers on albite surfaces during dissolution under hydrothermal conditions. *Geochim. Cosmochim. Acta* **54,** 1267–1281.

Hellmann R., Schott J., Dran J.-C., Petit J.-C., and Della Mea D. (1990b) A comparison of the dissolution behavior of albite and albite glass under hydrothermal conditions. *Geol. Soc. Amer. Ann. Mtg. Abstr., (abstr.)* p.A292.

Hochella M. F., Jr., Ponader H. B., Turner A. M., and Harris D. W. (1988) The complexity of mineral dissolution as viewed by high resolution scanning Auger microscopy: Labradorite under hydrothermal conditions. *Geochim. Cosmochim. Acta* **52,** 385–394.

Inskeep W. P., Nater E. A., Bloom P. R., Vandervoort D. S., and Erich M. S. (1991) Characterization of laboratory weathered labradorite surfaces using X-ray photoelectron spectroscopy and transmission electron microscopy. *Geochim. Cosmochim. Acta* **55,** 787–800.

Lanford W. A., Davis K., Lamarche P., Laursen T., and Groleau R. (1979) Hydration of soda-lime glass. *J. Non-Cryst. Solids* **33,** 249–266.

Lee M. R. and Parsons I. (1995) Microtextural controls of the weathering of perthitic alkali feldspars. *Geochim. Cosmochim. Acta* **59,** 4465–4488.

Lee R. R., Leich D. A., Tombrello T. A., Ericson J. E., and Friedman I. (1974) Obsidian hydration profile measurements using a nuclear reaction technique. *Nature* **250,** 44–47.

Machesky M. L. (1990) Influence of temperature on ion adsorption by hydrous metal oxides. In *Chemical Modeling of Aqueous Systems II* (ed. D. C. Melchior and R. L. Bassett); *ACS Symp. Ser.* **416,** 282–292. Amer. Chem. Soc.

Machesky M. L. and Jacobs P. F. (1991) Titration calorimetry of aqueous alumina suspensions Part II. Discussion of enthalpy changes with pH and ionic strength. *Colloids Surf.* **53,** 315–328.

Machesky M. L., Palmer D. A., and Wesolowski D. J. (1994) Hydrogen ion adsorption at the rutile-water interface. *Geochim. Cosmochim. Acta* **58,** 5627–5632.

Muir I. J., Bancroft G. M., and Nesbitt H. W. (1989) Characteristics of altered labradorite surfaces by SIMS and XPS. *Geochim. Cosmochim. Acta* **53,** 1235–1241.

Muir I. J., Bancroft G. M., Shotyk W., and Nesbitt H. W. (1990) A SIMS and XPS study of dissolving plagioclase. *Geochim. Cosmochim. Acta* **54,** 2247–2256.

Nesbitt H. W., Macrae N. D., and Shotyk W. (1991) Congruent and incongruent dissolution of labradorite in dilute acid, salt solutions. *J. Geol.* **99,** 429–442.

Pederson L. R., Baer D. R., McVay G. L., and Engelhard M. H. (1986) Reaction of soda-lime silicate glass in isotopically labelled water. *J. Non-Cryst. Solids* **86,** 369–380.

Petit J.-C., Della Mea G., Dran J.-C., Schott J., and Berner R. A. (1987) Mechanism of diopside dissolution from hydrogen depth profiling. *Nature* **325,** 705–707.

Petit J.-C., Dran J.-C., Della Mea G., and Paccagnella A. (1989a) Dissolution mechanisms of silicate minerals yielded by intercomparison with glasses and radiation damage studies. *Chem. Geol.* **78,** 219–227.

Petit J.-C., Dran J.-C., Paccagnella A., and Mea G. D. (1989b) Structural dependence of crystalline silicate hydration during aqueous dissolution. *Earth Planet. Sci. Lett.* **93,** 292–298.

Petit J.-C., Dran J.-C., Schott J., and Della Mea G. (1989c) New evidence on the dissolution mechanisms of crystalline silicates by MeV ion beam techniques. *Chem. Geol.* **76,** 365–369.

Petit J.-C., Della Mea G., Dran J.-C., Magonthier M.-C., Mando P. A., and Paccagnella A. (1990a) Hydrated layer formation during dissolution of complex silicate glasses and minerals. *Geochim. Cosmochim. Acta* **54,** 1941–1955.

Petit J.-C., Dran J.-C., and Della Mea G. (1990b) Energetic ion beam analysis in the Earth sciences. *Nature* **344,** 621–626.

Schindler P. W. and Kamber H. R. (1968) Die Acidität von Silanolgruppen. *Helv. Chim. Acta* **51,** 1781–1786.

Schoonen M. A. A. (1994) Calculation of the point of zero charge of metal oxides between 0 and 350°C. *Geochim. Cosmochim. Acta* **58,** 2845–2851.

Schweda P. and Sjöberg L. (1997) Near surface composition of acid-leached labradorite investigated by SIMS. *Geochim. Cosmochim. Acta* **61,** (in press).

Shotyk W. and Nesbitt H. W. (1992) Incongruent and congruent dissolution of plagioclase feldspar: Effect of feldspar composition and ligand complexation. *Geoderma* **55,** 55–78.

Sigg L. (1973) Untersuchungen über Protolyse und Komplexbildung mit zweiwertigen Kationen von Silikageloberflächen. M. Sc. thesis, Univ. Bern.

Sjöberg L. (1989) Kinetics and non-stoichiometry of labradorite dissolution. In *Proc. 6th Intl. Symp. on Water-Rock Interaction WRI-6* (ed. D. L. Miles), pp. 639–642. A. A. Balkema.

Sjöberg L., Strandh H., and Schweda P. (1995) Diffusion of protons and cations in leached feldspar surface layers. *EUG 8 Abstr.* **7,** 65.

Stillings L. L. and Brantley S. L. (1995) Feldspar dissolution at 25°C and pH 3: Reaction stoichiometry and the effect of ionic strength. *Geochim. Cosmochim. Acta* **59,** 1483–1496.

Stillings L. L., Brantley S. L., and Machesky M. L. (1995) Proton

adsorption at an adularia feldspar surface. *Geochim. Cosmochim. Acta* **59,** 1473–1482.

Sweeney R. J., Prozesky V. M., and Springhorn K. A. (1997) Use of the elastic recoil detection analysis (ERDA) microbeam technique for the quantitative determination of H in materials and H-partitioning between olivine and melt at high pressures. *Geochim. Cosmochim. Acta* **61,** 101–113.

Tirira J., Trocellier P., Forntier J. P., and Trouslard P. (1990) Theoretical and experimental study of low-energy ^{4}He-induced ^{1}H elastic recoil with application to hydrogen behaviour in solids. *Nucl. Instrum. Meth. Phys. Res.* **B45,** 203–207.

Wolery T. J. (1992) EQ3NR, A Computer Program for Geochemical Aqueous Speciation-Solubility Calculations: Theoretical Manual, User's Guide, and Related Documentation (Version 7.0). Lawrence Livermore Natl. Lab. UCRL-MA-110662 PT III.

Xiao Y. and Lasaga A. C. (1994) Ab initio quantum mechanical studies of the kinetics and mechanisms of silicate dissolution: H^+ (H_3O^+) catalysis. *Geochim. Cosmochim. Acta* **58,** 5379–5400.

Xiao Y. and Lasaga A. C. (1996) Ab initio quantum mechanical studies of the kinetics and mechanisms of quartz dissolution: OH^- catalysis. *Geochim. Cosmochim. Acta* **60,** 2283–2295.